VOLUME 19, 1957/58, No. 2 pp. 41-72 Published 24th August 1957

Philips Technical Review

DEALING WITH TECHNICAL PROBLEMS
RELATING TO THE PRODUCTS, PROCESSES AND INVESTIGATIONS OF
THE PHILIPS INDUSTRIES

AUDIO AMPLIFIERS WITH SINGLE-ENDED PUSH-PULL OUTPUT

by J. RODRIGUES de MIRANDA.

621.375.2.029.3

For some time now radio receivers have been available in which the loudspeaker is directly driven by the output valves, without the use of an output transformer. This means the omission of a component that, apart from adding to the losses and distortion, is quite expensive even to satisfy only moderate demands. The phase shift it introduces, moreover, prevents feedback being applied to its full advantage. This article deals with a new transformerless circuit for the last two stages of audio-frequency amplifiers which differs appreciably from the conventional one and can satisfy far higher demands. No expensive components are required to replace the transformer.

Music reproduction in the home of gramophone records, tape recordings or F.M. transmissions, may nowadays reach a very high quality indeed. If the excellent properties of such "music sources" are to be done full justice, the reproduction installation must come up to very high standards. Particularly in the last few years, therefore, there has been a general trend towards improvement of the reproduction system. This may consist of one or more loudspeakers and an audio-frequency amplifier, connected to a pick-up, the play-back head of a tape recorder, or to the R.F. and I.F. stages of an F.M. receiver.

Confining ourselves to the audio amplifier and the loudspeaker alone, there are three aspects to be considered, viz. the electronic circuitry, the loudspeaker design, and the acoustics.

The last two aspects were dealt with at some length in a recent article in this Review on a high-fidelity loudspeaker installation [1]). The present article is mainly concerned with the electronic aspects, i.e. with circuit development. As we shall see presently, this work has been influenced by certain innovations in the loudspeaker field.

The demands made on audio-frequency amplifiers involve the output power, frequency response, non-linear distortion and output resistance.

As regards frequency-response characteristics, it is not sufficient if merely the *amplitude* characteristic is flat within the audible range (20-18 000 c/s), since then the *phase* characteristic would possess the appropriate form only within a far narrower range; by the "appropriate" form is meant that the phase angle is proportional to the frequency (the proportionality factor may also be zero). With a poor phase characteristic a sudden burst of music, sharp consonants, etc. cannot be reproduced without distortion [2]). A good phase characteristic can be obtained if the amplitude characteristic remains flat far beyond the audible range, e.g. up to 40 kc/s. However, it is usually considered desirable to be able to vary the amplitude characteristic at either end of the audio band, i.e. have a tone control — preferably independent — of both the high and low notes.

Non-linear distortion in an amplifier is due to the non-linear characteristics of valves and magnetic materials. It gives rise to harmonics, which alter the timbre of the sound, and, worse, when two or more tones are produced simultaneously, to non-harmonic overtones (intermodulation). Non-linear distortion, rapidly increasing with amplitude above a certain signal strength, puts a definite limit to the maximum output power at which the amplifier can be satisfactorily operated.

---

[1]) G. J. Bleeksma and J. J. Schurink, A loudspeaker installation for high-fidelity reproduction in the home, Philips tech. Rev. **18**, 304-315, 1956/57 (No. 10).

[2]) See e.g. J. Haantjes, Judging an amplifier by means of the transient characteristic, Philips tech. Rev. **6**, 193-201, 1941.

Finally, the output resistance of the amplifier should be low, in order to provide a substantial damping effect on the loudspeaker, the latter having a mechanical resonance in the region of the very low notes [3]).

The designer of the amplifier has to try to satisfy these demands on characteristics, distortion and output resistance, whilst keeping the costs as low as possible. Considerations of price may carry considerable weight where mass production, e.g. of radio sets, is concerned. A low cost price is closely related to a high efficiency, for a poor efficiency involves a larger power pack and unnecessarily high-power output valves.

As output valve, the pentode is generally preferred to the triode, the former having a higher efficiency and requiring a smaller input signal. With a pentode, maximum efficiency (theoretically 50%) is obtained if the load resistance R_0 equals the D.C. resistance R_{ak} of the valve ($R_{\mathrm{ak}} = V_{\mathrm{a(w)}}/I_{\mathrm{a(w)}}$, $V_{\mathrm{a(w)}}$ and $I_{\mathrm{a(w)}}$ being the anode voltage and the anode current at the working point; R_{ak} should not be confused with the (much higher) internal resistance $R_{\mathrm{i}} = \partial V_{\mathrm{a}}/\partial I_{\mathrm{a}}$ at constant control-grid voltage). For most output pentodes R_{ak} has a value of several thousands of ohms.

A moving-coil loudspeaker of conventional design has a speech-coil of relatively few turns of fairly thick wire. Its impedance (virtually a resistance) is accordingly low, e.g. 7 Ω. This low impedance is matched to the far higher value of R_{ak} via a step-down output transformer. This component requires a great deal of care and material in its construction. Its stray self-inductance forms together with stray capacitances one or more oscillatory circuits, which impose an upper limit to the frequency range that can be reproduced. This cut-off frequency is the higher as the stray field and the winding capacitance are smaller, and therefore as the number of turns is smaller. One essential requirement for a good reproduction of the *low* notes, however, is a large primary self-inductance, which means a large number of turns. Another unfavourable factor is the fact that the anode direct current pre-magnetizes the core of the transformer.

The latter difficulty is avoided if a push-pull output stage is employed; D.C. magnetization of the core is then absent and a more favourable compromise between large primary self-inductance and small stray field and capacitance can be reached. A push-pull arrangement has furthermore the well-known advantage of producing less distortion: if the circuit is symmetrical, no even harmonics occur in the output signal. The complications incurred by using a second output valve (with the necessary phase-inverting element for getting two equal driving voltages in phase opposition), make the circuit more expensive, but for better-quality radio receivers and amplifiers the above advantages of push-pull operation outweigh the difference in price.

Apart from limiting the frequency range at both ends, the output transformer has the drawback of causing a loss of output power. Its efficiency is often as low as 50%, and seldom better than 80%, dependent upon the amount of material (and hence the cost) spent on it. The same applies to the distortion it introduces as a result of the non-linear *B-H*-curve of the iron core; here too, improvement can be reached only at the expenditure of more material.

Most serious of all, perhaps, is the fact that the output transformer prevents *negative feedback* being applied to its full advantage. With the aid of negative feedback, as is well known, the amplitude characteristic can be improved, the non-linear distortion reduced, and the output resistance lowered. If the circuit contains a phase-shifting element, however, such as an output transformer, which may act either inductively or capacitatively, there is a risk that for a given frequency the negative feedback aimed at becomes a positive feedback. To prevent instability, the feedback thus cannot be made as strong as might be desired.

As a consequence of all the difficulties mentioned above one is compelled to use a heavy and large (and hence expensive) output transformer, unless lower demands are made.

Some years ago Philips started working in another direction, viz. avoiding an output transformer altogether. If this attempt were to succeed, it would be possible, not only to eliminate all these drawbacks, but also to get rid of an expensive, bulky and heavy component. That these attempts have, in fact, been successful will appear from the following.

High resistance loudspeakers

Loudspeaker speech-coils having few turns of fairly thick wire have the advantage of being quickly wound, with little risk of breaking the wire, and also that the insulation of the wire takes up relatively little winding space (high filling factor).

The first investigations were aimed at establishing the largest number of turns and the smallest wire diameter that could be accommodated in the available space without unduly complicating manufacture or making the filling factor too small. Supported by their experience with all kinds of miniature winding jobs, the Eindhoven loudspeaker factory succeeded in 1953 in mass-producing 4000 Ω coils using 40 μ copper wire. These coils were provided with a central tapping, so that they could be directly incorporated in a push-pull circuit (*fig. 1*). The resistance of 2000 Ω for each half coil is fairly low for ordinary output valves, but is a practicable value for the UL 41 valve with its rather low D.C. resistance [4]). Both direct tests and life tests proved satisfactory, and part of the production of the radio receiver BX 521 U was equipped with such a loudspeaker, so that practical experience on a large scale could be gained. As regards the loudspeakers, no complaints were received. A remarkable feature of this set was the improved reproduction of the low notes.

---

[3]) See the article quoted in [1]), page 314.

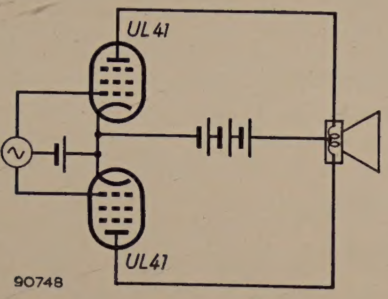

Fig. 1. Output stage with two pentodes UL 41 and a split-coil loudspeaker (type 9754) without output transformer. The resistance of the speech coil is 2 × 2000 ohms.

This solution, however, has its drawback. The output valves are operated as a Class A amplifier, i.e. with a large anode direct current. This current flows through the high-resistance loudspeaker coil, causing a considerable voltage drop (far greater than in an output transformer), and a considerable development of heat. In a new circuit, described below, these disadvantages have been completely eliminated.

The single-ended push-pull circuit

Fig. 2a shows a normal push-pull circuit. Each of the valves has been biassed to give a quiescent anode current $I_{a(w)}$. The supply, at a voltage V_b, therefore delivers a power $2V_bI_{a(w)}$. Fig. 2*b* shows a somewhat modified circuit, in which each valve again has the supply voltage V_b and the current $I_{a(w)}$, the total D.C. power being likewise $2V_bI_{a(w)}$. If the load resistance R_0 is the same in either case, the efficiency is also the same and the circuit of fig. 2*b* can supply the same A.C. power as that of fig. 2*a*.

This remains valid if *PP'* and *QQ'* in fig. 2*b* are interconnected. The two resistances R_0 are then connected in parallel and are equivalent to a single resistance $\frac{1}{2}R_0$ (fig. 2*c*), i.e. $\frac{1}{4}$ of the total resistance $2R_0$ of the circuit in fig. 2*a*. If the two valves are equally biassed, direct current flows only through the circuit formed by the supply source (voltage $2V_b$) and the two series-connected valves, none passing through the resistance $\frac{1}{2}R_0$.

This type of push-pull circuit was already well known in 1951 [5]). Clearly, it is ideally suited to the system of direct power transfer: it requires a 4 times lower load impedance than the conventional push-pull circuit, whilst owing to the fact that the load is free of direct current, all drawbacks such as large

---

[4]) Valves of the U-series are designed for universal A.C./D.C. receivers without mains transformer. They therefore have a low anode voltage (100-170 V), so that output valves of the U-series have to be designed for handling a large current. Their D.C. resistance R_{ak} is accordingly low.

[5]) A. Peterson and D. B. Sinclair, A single-ended push-pull audio amplifier, Proc. Inst. Rad. Engrs. **40**, 7-11, Jan. 1952.

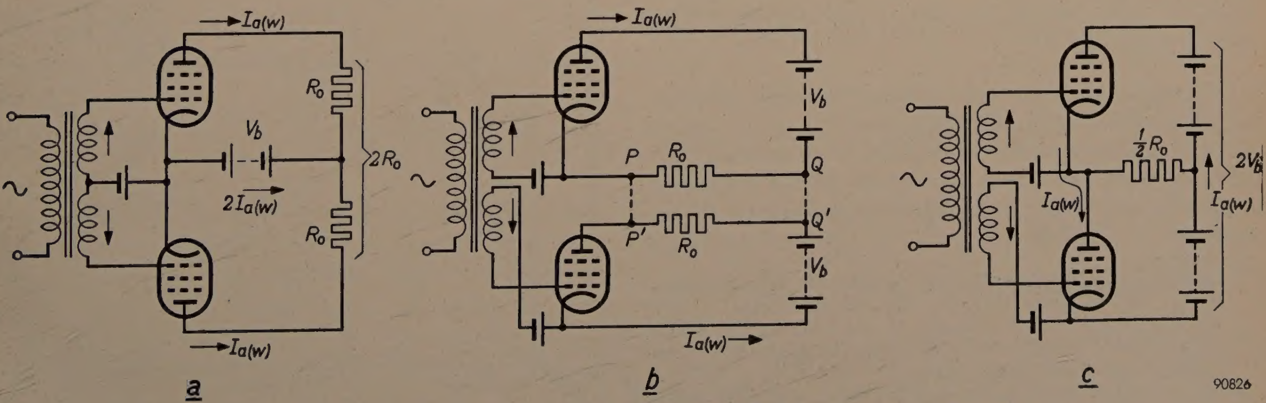

Fig. 2. *a*) Conventional push-pull circuit. *b*) Circuit which is electrically equivalent to (*a*). By interconnecting *P* and *P'* and *Q* and *Q'*, the single-ended push-pull circuit (*c*) is obtained, which matches to a 4 times lower load resistance ($\frac{1}{2}R_0$ instead of $2R_0$), whilst no D.C. flows through the load.

voltage losses and heat development in the loudspeaker coil are eliminated. The latter, moreover, does not require a central tapping, which simplifies manufacture. The central tapping of the supply source can likewise be eliminated, e.g. by connecting the loudspeaker L in series with a capacitor C_0 of sufficiently large capacitance according to *fig. 3.* Another method will be discussed presently.

The above principle has been applied in an increasing number of Philips receivers during the last few years. A new output pentode (type EL 86) has been developed for it, which can operate at low anode voltage and large anode current [6]); at maximum anode dissipation, the D.C. resistance R_{ak} amounts to only 1600 Ω. For the two valves, this requires matching by a loudspeaker impedance (mainly resistive) of 800 Ω, which presents no difficulties in manufacture. A single-ended push-pull circuit with two EL 86 valves can produce a maximum A.C. power of 10 W; for 10-20 W two EL 86 valves may be connected in parallel on either side, the required load resistance then being 400 Ω, which may be realized by using one 400 Ω loudspeaker or two 800 Ω loudspeakers in parallel. Nearly all Philips loudspeakers with a cone diameter of 12.5 cm and larger are now available in 400 or 800 Ω versions [7]).

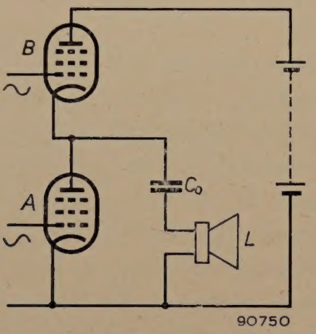

Fig. 3. Single-ended push-pull circuit with two pentodes A, B (EL 86) requiring no central tapping of the H.T. supply. A large capacitor C_0 is placed in series with the speech coil of loudspeaker L.

The relations between load resistance R_0, output power P_0 and the position of the operating point $V_{a(w)}$, $I_{a(w)}$ can be determined from the following simplified considerations. *Fig. 4* again shows the circuit of fig. 3 but with voltage and current indications added. The load resistance is here denoted R_0; the reactance of C_0 will be neglected. *Fig. 5* shows two idealized I_a-V_a characteristics of the pentodes employed. One characteristic is valid for a control-grid voltage $V_{g1} = 0$ and the other for the value of V_{g1} where $I_{a(w)}$ is half as large. XY is the load line intersecting the knee of the upper characteristic and subtending an angle a with the V_a axis such that cot a $= 2R_0$, this being the most favourable load line (i.e. a load of $2R_0$ for each valve; being in parallel, this gives a net load of R_0 as in fig. 4). It intersects the V_a axis at the point Y, corresponding to the voltage $2V_b$ of the supply source. The working point is W. We see that the relation cot $a = (2V_b - V_{a(w)})/I_{a(w)}$ is also valid; by neglecting the "knee voltage" $V_{a_{\min}}$ below which V_a must not drop, we have $2V_b = 2V_{a(w)}$ and therefore cot $a = V_{a(w)}/I_{a(w)}$. By definition, cot $a = 2R_0$ and $V_{a(w)}/I_{a(w)} = R_{ak}$, so that the matching condition $2R_0 = R_{ak}$ is satisfied.

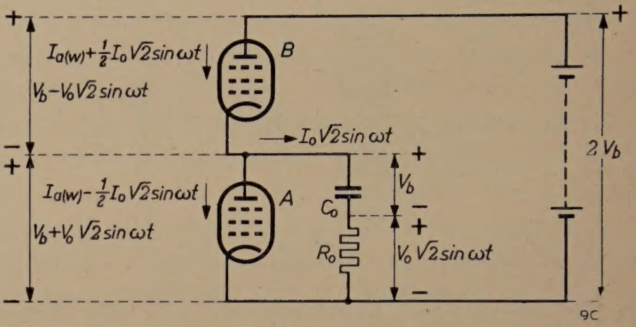
+
+
−
+
−
$I_{a(w)}+\frac{1}{2}I_0\sqrt{2}\sin\omega t$
$V_b-V_0\sqrt{2}\sin\omega t$
B
$I_0\sqrt{2}\sin\omega t$
$I_{a(w)}-\frac{1}{2}I_0\sqrt{2}\sin\omega t$
$V_b+V_0\sqrt{2}\sin\omega t$
A
C_0
R_0
V_b
$V_0\sqrt{2}\sin\omega t$
$2V_b$
9C

Fig. 4. Circuit of fig. 3 showing currents and voltages. A load resistance R_0 represents the loudspeaker.

The r.m.s. values of the alternating current I_0 and the alternating voltage V_0 are given by:

$$I_0 = \sqrt{P_0/R_0}, \quad V_0 = \sqrt{P_0 R_0}. \quad \ldots \ldots \quad (1)$$

Either valve contributes half the amount of I_0. The valve currents are $I_{a(w)} \pm \frac{1}{2}I_0\sqrt{2}$ sin ωt (see fig. 4). Under conditions of full drive (maximum signal), the entire load line XY is traversed, I_a swinging from zero to $2I_{a(w)}$. Therefore

$$I_{a(w)} = \tfrac{1}{2}I_0\sqrt{2}. \quad \ldots \ldots \ldots \quad (2)$$

V_a swings from $V_{a_{\min}}$ (approx. zero) to $2V_b$, so that

$$V_{a(w)} = V_0\sqrt{2}. \quad \ldots \ldots \ldots \quad (3)$$

For the voltage $2V_b$ of the H.T. supply, we thus have

$$2V_b = 2V_{a(w)} = 2V_0\sqrt{2}. \quad \ldots \ldots \quad (4)$$

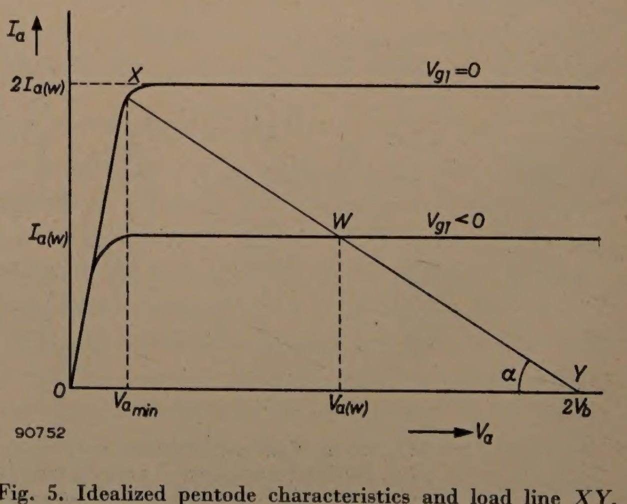

Fig. 5. Idealized pentode characteristics and load line XY. The working point is W.

---

[6]) As was recently pointed out in this Review (K. Rodenhuis *et al.*, Philips tech. Rev. **18**, 185, 1956/57, No. 7), such conditions are more favourable to the working life of the valve than when the same dissipation is obtained at a higher voltage and a smaller current.

[7]) 800 Ω speakers are designated by the suffix A, 400 Ω speakers by the suffix B to the type number, e.g. 9710 A, 9766 BM; the suffix M indicating a double-cone loudspeaker (see J. J. Schurink, Philips tech. Rev. **16**, 241-249, 1954/55, or the article quoted by [1]), pp. 305-306).

The power P_b actually delivered by the source is

$$P_b = 2V_b I_{a(w)} = 2V_0\sqrt{2} \times \tfrac{1}{2}I_0\sqrt{2} = 2V_0 I_0 = 2P_0,$$

which demonstrates that the efficiency is 50%.

In the *absence* of a signal the supply delivers the same power $P_b = 2P_0$, which is now entirely dissipated in the valves, which means for each valve a dissipated power $P_0 = V_b I_{a(w)}$ (twice as much as under conditions of full drive). This means that the maximum A.C. power the circuit is permitted to deliver, is equal to the maximum anode dissipation in the absence of a signal. This quantity is a parameter of the valve, and amounts to 12 W for the EL 86. Owing to the simplifications introduced here, P_0 is actually somewhat lower, viz. 10 W.

For $P_0 = 10$ W and $R_0 = 800\ \Omega$, we arrive, according to (1), at $I_0 = 112$ mA and $V_0 = 90$ V. The working point of the valve now follows from (2) and (3):

$$I_{a(w)} = 79 \text{ mA}, \quad V_{a(w)} = 127 \text{ V}.$$

According to (4), the supply voltage must amount to $2V_b = 254$ V, to which must be added the amount $2V_{a_{\min}}$ (and, if the negative grid bias of valve A in fig. 4 is produced across a cathode resistor, an additional $|V_{g1}|$).

For maximum output powers lower than 10 W the valve may be biassed to give a smaller quiescent anode current at a proportionally lower supply voltage, the working point being evaluated in the above manner.

The signal to be amplified generally consists of a single alternating voltage with respect to earth. For driving the valves of a push-pull circuit in opposite phase, however, two control voltages are required. This could be obtained by means of a transformer with two secondary windings as shown in fig. 2*a* for the ordinary push-pull circuit and in fig. 2*c* for the single-ended push-pull circuit. For some time however, a valve (phase inverter) has been preferred to obtain the opposed control voltages for a conventional push-pull circuit. A valve can also be used for this purpose with a single-ended push-pull circuit, as is shown in *fig. 6*. Section I of a double-triode ECC 83 functions here as amplifier and is connected to the control grid of the output valve A (for the sake of clarity, coupling capacitors are not shown in the diagram) and also to the grid of section II. At the anode of II a signal in opposite phase is produced, which, by an appropriate choice of resistances, is given an amplitude suitable for driving output valve B.

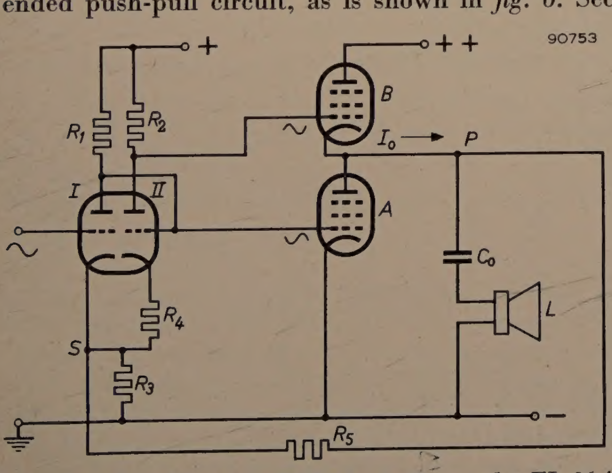

Fig. 6. *I-II* double-triode ECC 83. *A*, *B* pentodes EL 86 in single-ended push-pull arrangement. The first stage of the amplifier, consisting of triode *I*, drives the output valve *A* and the phase inverter *II* producing the control voltage for *B*. (Components not essential to the principle, such as coupling capacitors, are not shown.) Positive feedback in the first-amplifier - phase-inverter stage is effected via the common cathode resistor R_3 of *I* and *II*. Negative feedback, from *P* to *S*, is obtained via R_5.

Feedback

As mentioned earlier, one of the advantages of omitting an output transformer is the greater freedom in applying negative feedback. Without running the risk of instability, certain combinations of negative and positive feedback can even be made, by which, as we shall demonstrate presently, distortion can be drastically reduced. In the circuit of fig. 6 [8]) negative feedback is realized by passing part of the output current I_0 (being proportional to the output voltage), via resistor R_5, through cathode resistor R_3; at the same time there is positive feedback in the phase inverter stage in the form of valves I and II having resistor R_3 as a common cathode resistance.

The effect of combined positive and negative feedback is clearly demonstrated by a hypothetical example of greater simplicity than that of fig. 6. A_1 and A_2 in *fig. 7* represent two amplifiers in cascade, e.g. a pre-amplifying stage and an output stage, whose amplifications will likewise be called A_1 and A_2 respectively. A portion B_1V_1 of the output signal V_1 of A_1 is fed back to the input of A_1, and a portion B_2V_0 of the output signal V_0 of A_2 is likewise fed back to the input of A_1. If V_i is the signal to be amplified, we may write, quite generally,

$$V_1 = A_1(V_i + B_1V_1 + B_2V_0)$$

and

$$V_0 = A_2V_1.$$

The overall amplification A is accordingly:

$$A = \frac{V_0}{V_i} = \frac{A_1A_2}{1 - A_1B_1 - A_1A_2B_2} = \frac{A_1A_2}{N},$$

where

$$N = 1 - A_1B_1 - A_1A_2B_2.$$

Similarly, the total distortion D is given by

$$D = \frac{1}{N}D_1 + \frac{1 - A_1B_1}{N}D_2 + \frac{1 - A_1B_1}{N}D_1D_2,$$

---

[8]) Designed by E. H. Nielsen, formerly a member of the laboratory of the Philips factory in Copenhagen.

where D_1 and D_2 are respectively the distortion of either amplifier.

It may be seen that if A_1B_1 is made unity, a very special situation arises: D is reduced to D_1/N, i.e. the distortion of amplifier A_2 does not contribute at all to the total distortion. The remaining distortion, D_1/N, is determined by the (slight) distortion D_1 of the first amplifier and by the quantity N, the latter becoming $-A_1A_2B_2$ for $A_1B_1 = 1$. The absolute value of $A_1A_2B_2$ may be considerable larger than unity, in which case the total distortion D will even be appreciably smaller than D_1. Also, the absolute value of the total amplification A becomes equal to $1/B_2$ (and therefore independent of A_2).

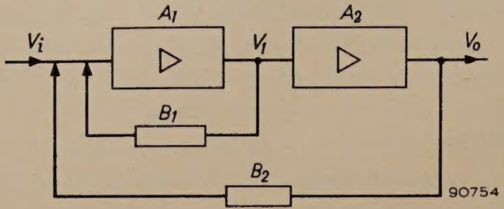

Fig. 7. Cascade connection of two amplifiers A_1 and A_2, the former having a feedback loop via B_1, and the combination a feedback via B_2.

The condition $A_1B_1 = 1$ can be fulfilled for a wide frequency range if A_1 and B_1 are real in that range, i.e. if the amplifier A_1 and the feedback circuit B_1 contain no phase-shifting elements. In the first amplifying stage this condition may be closely approached without any difficulty. This condition being fulfilled means that the amplifier A_1 is given such a positive feedback B_1 that it is on the verge of oscillating. This does not necessarily mean that the combination A_1-B_1-A_2-B_2 (fig. 7) is unstable; if the second amplifier and the feedback circuit are free of any elements causing adverse phase shifts, the whole circuit can be kept stable by applying a certain negative feedback B_2. An output transformer is an element which inevitably causes such phase shifts that the stability would be seriously jeopardized [9]). Only by its elimination is it possible to realize circuits of the type considered here.

Practical examples

A.F. amplifier for a radio receiver

Fig. 8 shows a further developed version of the circuit of fig. 6, as it might be used for a radio receiver. Here the feedback resistor R_5 of fig. 6 has been replaced by two networks, C_1-R_6-R_7 and C_2-R_8-R_9. These incorporate the tone controls: R_6 for the low and R_9 for the high notes.

---

[9]) The output transformer can be kept outside the feedback loop B_2 (see e.g. fig. 6 of the article quoted by [5])), but the distortion introduced by it remains undiminished in the output signal; also the degree of negative feedback is necessarily limited owing to the phase shift between primary voltage and primary current.

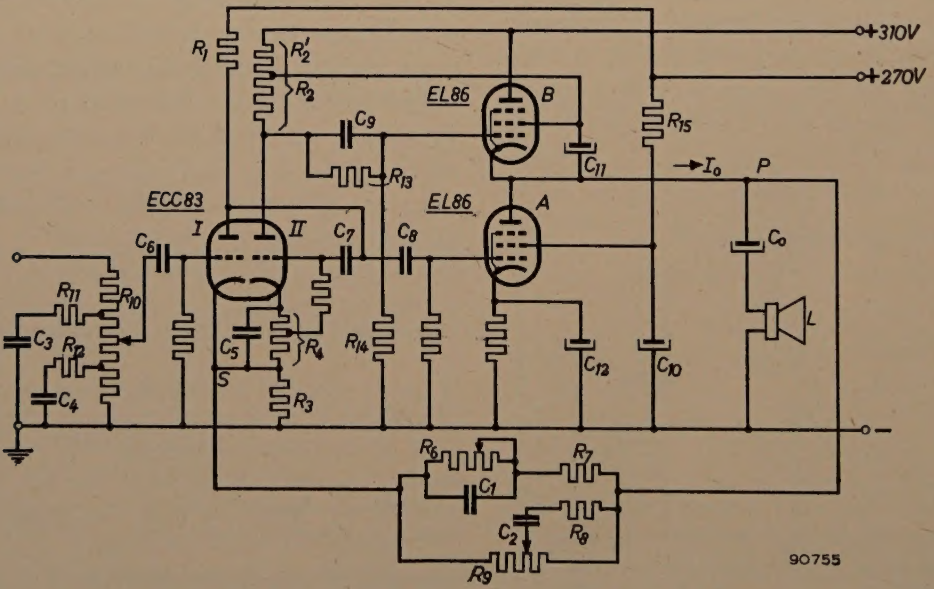

Fig. 8. More detailed version of the schematic diagram of fig. 6. Instead of the feedback resistor R_5, the networks C_1-R_6-R_7 and C_2-R_8-R_9 have been incorporated; R_6 low-note control, R_9 high-note control. R_{10} volume control with branches R_{11}-C_3 and R_{12}-C_4 for low-note compensation at low levels of volume. C_5 reduces the negative feedback through R_4 for the high audio frequencies. C_6, C_7, C_8, C_9 coupling capacitors. The voltage divider R_2-R_{13}-R_{14} provides the correct bias for the control grid of output valve B. The screen grid of the output valve A is fed via resistor R_{15} and the screen grid of B from a tapping on R_2 (for other methods of screen-grid supply, see figs. 11 and 12).

Low notes. Capacitor C_1 reduces the negative feedback at low frequencies, so that the latter are relatively more amplified. For a radio set this is a desirable feature, e.g. for compensating the drop in loudspeaker radiation at frequencies below those at which the cabinet forms a sufficiently large baffle. With a cabinet of average size, the drop in loudspeaker response at descending frequency (6 dB per octave) begins at about 1000 c/s. As desired, the effect of C_1 can be decreased (increasing the negative feedback and thus increasing low-note attenuation) by lowering the resistance of R_6. The non-variable resistor R_7 prevents the negative feedback becoming too strong.

High notes. The values of C_2 and R_8 are so chosen that the higher audio frequencies are mainly fed back through this branch. If the sliding contact on R_9 in fig. 8 is moved to the right, a larger part of R_9 is connected in series with this branch, the negative feedback diminishes and the high notes become accordingly stronger.

As is customary in many Philips receivers, automatic low-note compensation is provided at low levels of volume: volume control R_{10} is provided with the branches R_{11}-C_3 and R_{12}-C_4, which ensure that with a reduction of the total volume the low notes are relatively less attenuated, thus compensating for the property of the human ear of becoming insensitive to a steadily increasing portion of the low-note range when the volume is reduced.

Near the upper limit of the audio spectrum the amplification is reduced as a result of the anode capacitance of the output valves and of the Miller effect (reaction of anode upon control grid). This has been compensated by placing a capacitor C_5 across cathode resistor R_4 of the phase inverter. The effect of this is a reduction of the negative feedback in the phase-inverter stage, thus increasing the gain, particularly at the higher frequencies.

Figs. 9 and *10* give some idea of the results attained with an amplifier of the above type. The diagrams of fig. 9 show the distortion as a function of the output power for the frequencies 90, 1000 and 8000 c/s, whilst fig. 10 shows the amplitude-frequency characteristic with both tone controls set to maximum. It can been seen that the low and high notes are boosted with respect to the medium range, as is desirable for a radio receiver.

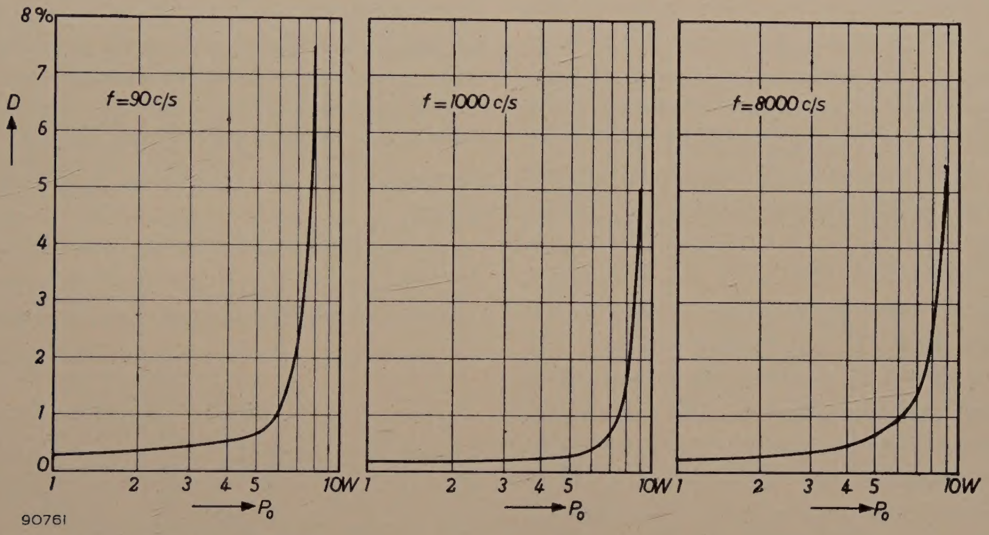

Fig. 9. Distortion D, measured on an amplifier of the type shown in fig. 8, plotted against the output power P_0, at the frequencies 90, 1000 and 8000 c/s. Both tone controls set to maximum.

As a measure of the sensitivity of an amplifier, it is customary to give the input r.m.s. voltage required to produce an output power of 50 mW at 1000 c/s. For this particular example this voltage amounts to 24 mV, which is normal for the audio section of a radio receiver.

Negative feedback reduces the internal resistance of the output stage to about 20 Ω, a value that is

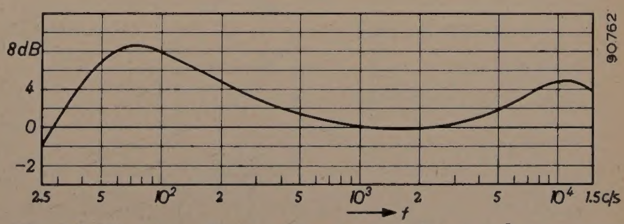

Fig. 10. Output voltage with constant input voltage versus frequency f, measured on an amplifier of the type shown in fig. 8, loaded with 800 ohms. Both tone controls set to maximum (i.e. minimum negative feedback). Boosting of the low and high notes as shown is desirable in the audio amplifier of a radio receiver.

low compared with the load resistance (800 Ω). This is conducive to the uniform reproduction of the very low notes (damping of the loudspeaker resonance).

With a single-ended push-pull circuit a question requiring attention is the supply for the screen grids of the output valves. The screen grid voltage should be at about the same D.C. level as the anode, but there must be no alternating voltage between screen grid and cathode.

Let us first investigate how this ideal condition can be approached with the output valve A (fig. 8). Here the screen grid is supplied via resistor R_{15}, whilst the electrolytic capacitor C_{10} (in series with C_{12}) constitutes a low impedance between screen grid and cathode. The screen-grid current (about 5 mA) forms only a minor portion of the average cathode current. This portion is not constant however: it varies with the amplitude of the signal on the control grid. The average value of the screen-grid current therefore varies with the signal strength, so that the presence of the series resistor R_{15} makes the screen-grid voltage vary with signal strength: the stronger the signal, the lower the screen-grid voltage. This effect reduces the maximum output power of the valve. To minimize the effect, the resistance R_{15} should be made as small as possible and the screen grid must therefore be fed from a source whose voltage exceeds the required value by as little as possible. For this reason the screen grid in fig. 8 is not fed from the 310 V source, but from the 270 V source (which also supplies the valve-half I and the R.F. part of the receiver). A supply direct from a voltage of approx. 155 V would be even better, and this can be easily realized if the 310 V supply is derived from a full-wave bridge circuit rectifier (*fig. 11*): if the secondary of the transformer is provided with a central tapping, half the direct voltage can be tapped off from this point.

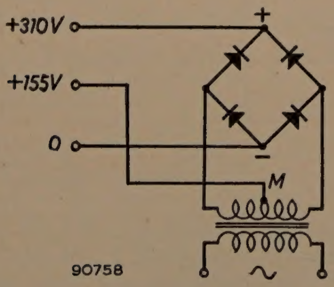

Fig. 11. Full-wave bridge circuit rectifier. Half the direct voltage can be obtained from the centre-tapping M on the secondary of the transformer. This can be used for feeding the screen grid of valve A in fig. 8.

As for the output valve B (fig. 8), its anode has a fixed potential, whilst the output signal voltage is taken off at the cathode. If the screen grid were connected directly to the anode, then the loudspeaker would be nearly short-circuited (for signal currents) via capacitor C_{11} and the H.T. supply. A certain impedance between screen grid and anode must therefore always be provided (unless a separate power supply is to be provided for this screen grid). This impedance should be high with respect to the (parallel) loudspeaker impedance, but, on the other hand, it should not have a high D.C. resistance, as otherwise the screen-grid voltage would be too much below the anode voltage and also would vary too much with the signal strength (see above). In some respects a choke has some advantages over a resistor, but this would again introduce a phase-shifting element. In fig. 8 a compromise has been struck between a not too high and not too low resistance by connecting the screen grid to a suitable tapping on the anode resistor R_2 of the phase inverter.

A more elegant solution is shown in *fig. 12*. Here the loudspeaker itself is connected between screen grid and anode. The output signal current I_0 passes without losses (with the exception of the part used for feedback) via C_{11} through the loudspeaker. The function of capacitor C_0 is now taken over by C_{11} and it can therefore be omitted. The fact that the (small) screen-grid current now flows through the loudspeaker forms no objection.

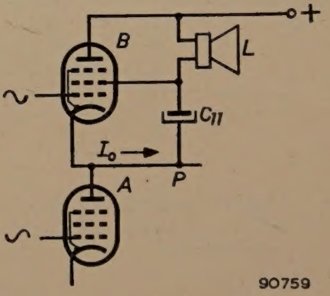

Fig. 12. Supply to the screen grid of valve B in fig. 8 via the loudspeaker L. The output current I_0 (less the negative-feedback current) flows through C_{11} and L.

Further improved circuit

The reader may have noted that in fig. 8, from which the output transformer with its phase-shifting effect has been eliminated, other phase-shifting elements have after all been included, viz. the tone control networks in the feedback circuit. In principle such a solution is indeed not ideal. That it is nevertheless used is justified by the fact that otherwise an additional amplifying stage would be required (the additional amplification of low and high notes is effected here by reducing the negative feedback), and by the fact that even with the smallest amount of negative feedback, distortion remains appreciably smaller than in a conventional circuit with the average output transformer.

If near-perfection is aimed at, then the negative feedback loop should be kept free from any phase shift by effecting the tone control in an additional stage preceding valve *I*. For an amplifier of this type the following distortion figures were measured:

Output power (in W)	10.4	9.25	4	1
Distortion (in %)	0.30	0.11	0.05	0.03

In order to obtain for this measurement an input signal itself sufficiently free of distortion, a filter for suppressing harmonics should be incorporated between the audio generator and the amplifier. Any harmonics in the output signal of the amplifier are measured with a "wave analyzer", by means of which each harmonic can be separately determined.

Fig. 13 shows the amplitude and phase characteristics of this amplifier. We see that the point where the amplification has dropped by 3 dB lies well into the ultrasonic range, namely at 250 kc/s, whilst the phase shift in the audible range is restricted to a few degrees only. For an output power of 10 W the efficiency of the output stage is a good 42%, which is very satisfactory. The only critical resistance value is that of the cathode resistor of the phase inverter (R_4), which must be accurate within 2%; for all other resistors a 10% tolerance is adequate.

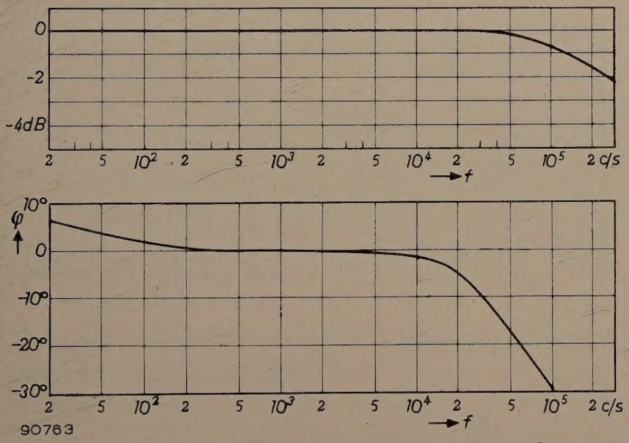

Fig. 13. Amplitude characteristic (above) and phase characteristic (below) of an improved single-ended push-pull amplifier.

We shall confine ourselves to the above two examples. It may be mentioned, however, that in many other cases the greater freedom in the application of negative feedback which single-ended push-pull makes possible will be welcome: it permits the realization of various types of special circuits for which the output transformer has hitherto formed the great stumbling block.

Summary. The low resistance of the speech coils of conventional moving-coil loudspeakers requires a transformer for matching to the far higher D.C. resistance of the output pentode. This output transformer has many disadvantages: it limits the reproduced audio spectrum on either end, causes power losses, introduces distortion, and by the phase-shift it introduces, prevents negative feedback being employed to its full advantage. Any transformer in which these drawbacks are confined within acceptable limits is necessarily a heavy, bulky and expensive component.

In 1953 Philips manufactured loudspeakers with a speech coil of 2 × 2000 ohms, which could be incorporated in a normal push-pull circuit with two pentodes UL 41. For such a "direct power transfer", however, the "single-ended push-pull circuit" is more suitable: here the load (loudspeaker) can have a resistance 4 times as low as with the conventional push-pull circuit, whilst no direct current flows through it. This led to the development of the output pentode EL 86, with a D.C. resistance of 1600 ohms at full load, and of associated loudspeakers of 800 and 400 ohms. Two valves EL 86 in single-ended push-pull can deliver 10 W.

The absence of an output transformer makes it possible to realize circuits in which the first amplifying stage has positive feedback up to the verge of oscillation, whilst the first amplifying stage and the output stage together have negative feedback. Such a circuit is perfectly stable. The total distortion can be reduced to only a small fraction of the distortion of the first amplifying stage alone and made independent of the distortion in the output stage. Two practical examples are discussed, one with the tone controls incorporated in the negative feedback circuit and one with the tone controls in a separate preceding stage. In the latter case the distortion at 10 W is only 0.30%; the amplitude characteristic remains straight well into the ultrasonic range before showing a 3 dB drop at 250 kc/s, so that the phase characteristic does not show deviations greater than a few degrees within the audible range.

STROBOSCOPIC OPERATION OF PHOTOMULTIPLIER TUBES

by C. F. HENDEE *) and W. B. BROWN *).

621.383.27

By applying pulse voltages instead of the usual D.C. voltages to the electrodes of a photomultiplier tube, such a tube is made to operate as a light shutter capable of shutter times of fractions of a microsecond. An interesting method for the analysis of very weak light flashes and for "time-resolved spectroscopy" is based on this type of operation. The behavior of the pulsed photomultiplier tube is in several respects different from that under D.C. operation.

Aim and principles of method

Multiplier phototubes, in which the electron current emitted by a photocathode under illumination is enormously amplified by secondary electron emission from a number of successive electrodes ("dynodes"), have found wide-spread application in modern physics and technology. A specialized field of great importance is scintillation counting, in which high energy particles or radiation quanta are detected, counted and their energy measured by means of the flash of light they produce in a scintillating crystal or liquid [1]). Equally important is the direct measurement of weak light sources, such as stars, spectral lines, etc. and of rapidly varying light sources, for instance in sound and facsimile reproduction [2]). The main characteristics utilized in such applications are the extremely high sensitivity of the photomultiplier tube and its extremely quick response: the time delay, given by the total transit time of electrons through the tube, amounts to a few 10^{-8} sec.

A special problem that will be discussed in this article and to which the photomultiplier tube is ideally suited, is the spectral study of weak light flashes, e.g. from electrical discharges in gases. Generally this has been done in the past by presenting the amplified output of a photomultiplier tube on an oscilloscope synchronized with the light flash. The oscilloscope trace will then indicate the time variation of the light intensity, either of the total light or of that in a specified spectral region if this is singled out by a monochromator and focused on to the photomultiplier tube.

With weak sources, and especially after spectral dispersion that may reduce the intensity to a minute fraction, one ultimately reaches in these studies a point where the whole signal to be detected and displayed is carried by a few photoelectrons [3]). This is clearly seen in *fig. 1* which shows that for the lowest light intensities the gradually varying magnitude of the signal is not represented by a gradually varying vertical displacement of the oscilloscope trace but rather by a variation of the "density" of separate photoelectron pips. The determination of the relative intensities and pulse shapes from such signals obviously will be rather difficult and the accuracy very poor.

The photomultiplier tube can be made to provide a very effective solution for this problem in the following manner. Since the tube is sensitive to light only when proper voltages are applied to the cathode and the dynodes, it can be made to operate as a *light-shutter* by applying these voltages during a well-defined period, i.e. in the form of a rectangular pulse. The "on" time of the tube can be restricted to say 10^{-7} sec and can be timed by suitable pulse techniques to occur at any desired phase of the light flash. The photocurrent obtained at the collector of the tube during the "on" time is fed to a D.C. microammeter, preferably of a recording type. If now the light flash is periodically repeated and the photomultiplier tube is pulsed always in the same relative phase, the pulsed photocurrent may be *integrated* over a suitably long period by having a long time constant in the current meter, without loss of information concerning the time variation of the light flash.

It will be recognized that this procedure is similar to the obtaining of a stationary image of periodic

---

*) Philips Laboratories, Irvington-on-Hudson, N.Y., U.S.A.

[1]) G. A. Morton, Photomultipliers for scintillation counting, RCA Rev. **10**, 525-553, 1949.
A. Krebs, Szintillationszähler, Ergebn. exakt. Naturwiss. **27**, 361-409, 1953.

[2]) See for instance R. W. Engstrom, Multiplier photo-tube characteristics: application to low light levels, J. Opt. Soc. Amer. **37**, 420-431, 1947.

[3]) R. F. Saxe, Detection and recording of optical transients by photo-multipliers, Nature (London) **172**, 1198, 1953.

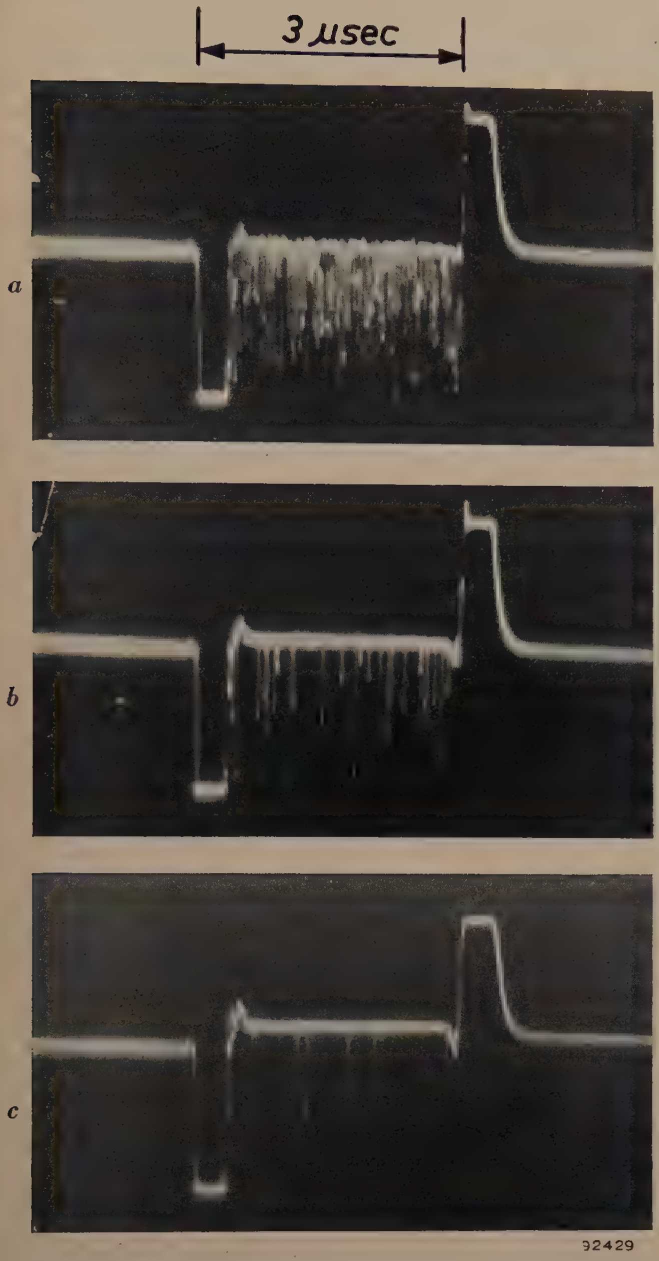

Fig. 1. Oscilloscope traces of the output of a photomultiplier tube subject to a very weak illumination, decreasing in intensity from (*a*) to (*c*). For reasons discussed later, the photomultiplier tube in each case was made to operate only during a short time, viz. 3 microseconds. During this time, only a few photoelectrons are produced with the lowest intensities. Owing to the random nature of the photon arrival and of the secondary electron emission process in the tube, the pips caused by separate photoelectrons occur at irregular intervals and differ greatly in amplitude.

The two large pips (one down on the left and the other up on the right of each trace) in this figure and also in figs. 8 and 9 result from capacitive pick-up at the photo-tube collector of the high-voltage pulse applied to the dynodes (cf. fig. 10).

processes by stroboscopic observation 4). The analogy is made complete when the phase of the photomultiplier tube is gradually shifted so as to *scan* the complete light pulse.

Apart from the ease of evaluation, the method provides a considerable increase in accuracy as compared with the measurement of a single flash: for very low intensity light, where the primary photocurrent in each pulse may consist of only a few (or even less than one, on the average) photoelectrons, the statistical variation of this number of photoelectrons and hence the probable error in the determination of intensity is relative large. Using repetition rates of the light flash of up to 10 000 per second and integration times up to 10 seconds, a number of photoelectrons 10^5 times larger than in a single flash can be accumulated, and the accuracy thereby improved by a factor of about 300. A more detailed discussion of this improvement will be given below.

Evidently the method can be used only for light sources which can give repetitive flashes. Many types of electrical discharges in gases permit periodic pulsing at high frequencies 5). Among the subjects investigated by this technique in the Philips Laboratories at Irvington is the light from a hydrogen thyratron and the light from low-pressure discharges in nitrogen. In most cases light flashes of 1 microsecond duration were used. The set-up for the measurements, using a monochromator, is shown schematically in *fig. 2*; a photograph of the equip-

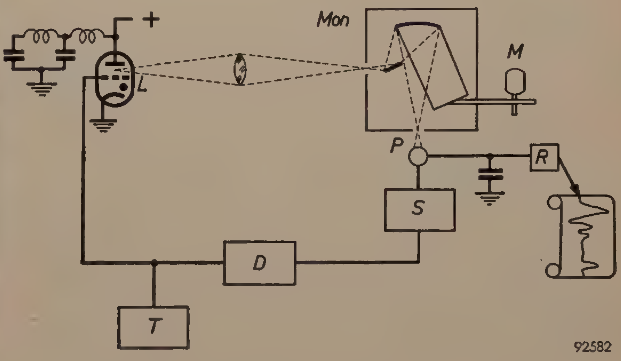

Fig. 2. Set-up for time-resolved spectroscopy using a stroboscopically operated photomultiplier tube. *T* trigger circuit, *L* pulsed light source to be analyzed (in this case a hydrogen thyratron), *Mon* grating monochromator with motor drive *M*, *S* circuit providing the pulse voltages for the photomultiplier tube *P*, *D* variable delay circuit, *R* recording D.C. microammeter.

In most experiments described in this article the RCA photomultiplier tube 1 P 21 was used.

---

4) C. F. Hendee, Time-resolved spectroscopy with pulsed photomultipliers, J. Opt. Soc. Amer. **43**, 330, 1953 (abstract). C. F. Hendee and W. B. Brown, Time-resolved spectroscopy of nitrogen and hydrogen, Phys. Rev. **93**, 651, 1954 (abstract).
A similar technique for longer pulses is described by A.V. Phelps and J. L. Pack, Measurement of time varying optical absorption, Rev. sci. Instr. **26**, 45-49, 1955.

5) C. F. Hendee, Band spectra in pulsed nitrogen discharges, Phys. Rev. **84**, 1075, 1951 (abstract). Cf. also R. D. Drosd, Gated multiple light pulse generator, Bull. Amer. Phys. Soc. **30**, No. 4, p. 36, 1955 (abstract).

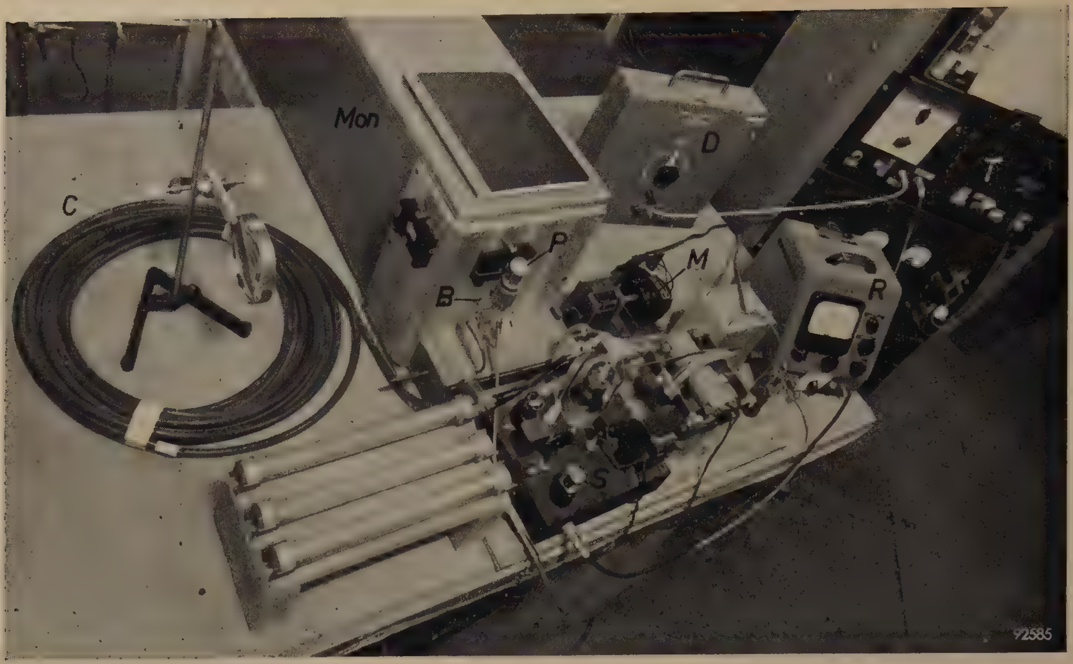

Fig. 3. Photograph of equipment outlined in fig. 2. Same lettering as in fig. 2. The light source is to the left (not visible). To the right, a rack containing the trigger circuit T and the recording part of the current meter R is seen. C is a length of coaxial cable acting as a pulse forming network in the circuit S. B are the voltage-divider resistors for the photomultiplier-tube dynodes (see fig. 10).

ment is seen in *fig. 3*. In order to determine the time variation of the intensity of a particular spectral line during a flash, the monochromator setting was fixed on this line and the short photomultiplier pulse was slowly phased through the light flash by means of the variable delay circuit, D in fig. 2. A record is thus obtained on the strip chart recorder which represents the light intensity as a function of time ⁶). *Fig. 4* is such a record showing part of the pulse shape of two hydrogen lines in the light emitted by a pulsed hydrogen thyratron. Alternatively a complete spectrum of the light can be recorded at particular instants of the flash time with an approp-

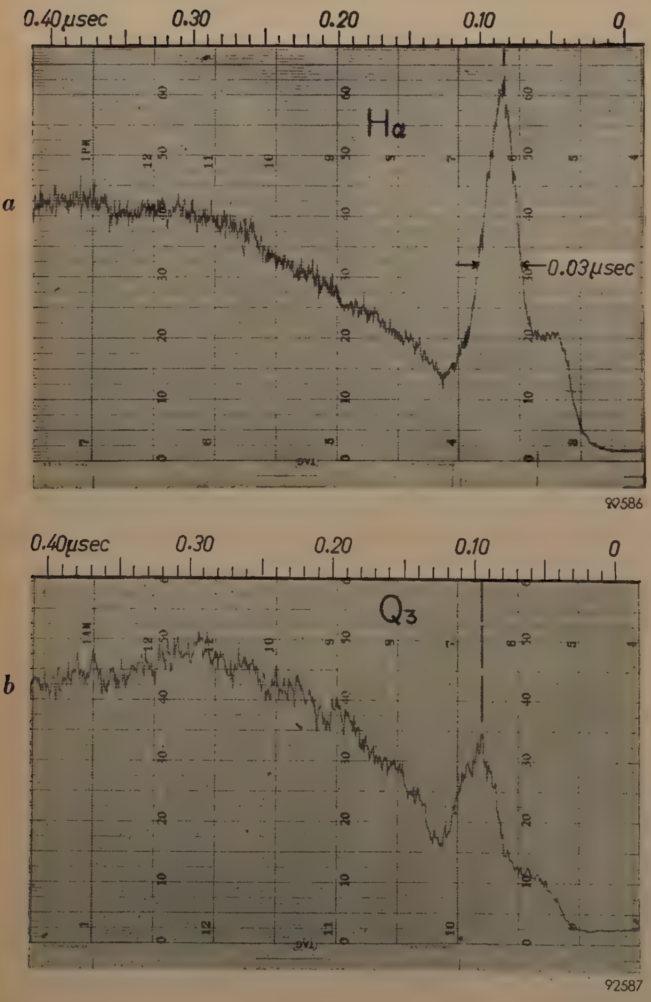

Fig. 4. Part of the pulse shape of two hydrogen lines in the spectrum radiated by a 4 C 35 hydrogen thyratron during a 1.0 microsecond pulse and analysed by the method described. The time scale runs from right to left in this figure. *a*) Line at 6563 Å emitted by atomic hydrogen. *b*) Line at 6032 Å belonging to the $3p^3\Pi - 3s^3\Sigma$, 0—0 band emitted by the hydrogen molecule.

The records are not typical of hydrogen thyratron pulses but were obtained in a case when there was a large current spike early in the 1 µsec pulse. The dynode voltage pulses used for scanning the 1 µsec light pulse duration had a measured length of 9×10^{-8} sec.

---

⁶) Proper attention, of course, must be given to the selection of the scanning time; the problem is similar to that described in some detail in this Review for the analogous case of the scanning of X-ray diffraction patterns: see W. Parrish, X-ray intensity measurements with counter tubes, Philips tech. Rev. 17, 206-221, 1955/56.

riate fixed setting of the delay circuit and scanning of the spectrum with the motor-driven monochromator ("time-resolved spectroscopy"). *Fig. 5* shows a portion of the hydrogen band spectrum, emitted 0.2 μsec after the initiation of the discharge, which was obtained in this fashion. *Fig. 6* is a series of spectra from a nitrogen discharge (duration of the electrical discharge 10^{-7} sec) demonstrating the rapid changes in the spectrum that may occur within a fraction of a microsecond. Such changes are due to differences in excitation and life of the molecules in the quantized energy levels participating in the emission of the various lines and bands.

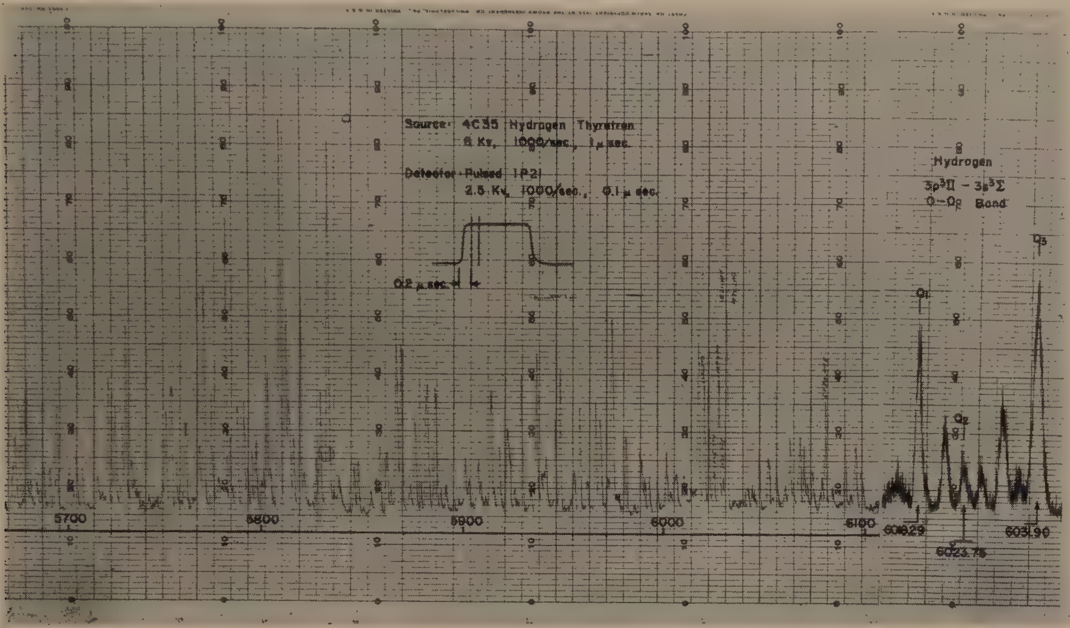

Fig. 5. Time-resolved spectroscopy: part of the hydrogen band spectrum emitted from a 4 C 35 hydrogen thyratron 0.2 μsec after initiation of a 1.0 μsec square current pulse. Thyratron peak voltage 6 kV, pulse repetition rate 1000 per sec. Right: narrow part of the spectrum recorded with greater dispersion.

Behavior of the photomultiplier tube under pulsed operation

An essential factor in these experiments is the internal *gain* of the photomultiplier tube. Much higher gains can be achieved under pulsed operation than with D.C. voltages on the tube, owing to the fact that higher voltages are permissible. This remarkable fact has been known and made use of for some time [7]. The oscillograms of single light flashes in fig. 1 in fact were obtained with a pulsed 1 P 21 photomultiplier tube at a voltage of 1500 V, since the gain of this tube under normal operation (maximum D.C. voltage 1230 V) would not have been sufficient to render visible each separate photo electron.

The gain was determined and its variation with voltage studied by means of a series of pictures similar to fig. 1, made under constant illumination. The average number $\bar{n}_p$ of photoelectrons per pulse was counted and the gain g calculated from the photomultiplier pulse repetition rate f and the measured average collector current $\bar{I}_p$, using the equation:

$$\bar{I}_p = \bar{n}_p f g e, \quad . \; . \; . \; . \; . \; . \quad (1)$$

e being the electronic charge. Within the admissible D.C. voltage range, the gains under D.C. and pulsed conditions were found to be equal. The gain under pulsed operation continued to grow as the voltage was increased, until a value of 0.8×10^9 was reached at 2500 volts (total voltage on the tube, i.e. between cathode and collector, the dynodes being supplied with equally spaced intermediate voltages taken from a potentiometer; cf. fig. 10). This is illustrated by *fig. 7*.

Incidentally, the oscillograms of fig. 1 neatly illustrate the effective shutter action of the pulsed photomultiplier tube: no signal whatever appears before or after the pulse. Practically all the pips occurring during the pulse are due to photoelectrons:

---

[7] R. F. Post and N. S. Shiren, Performance of pulsed photomultiplier scintillation counters, Phys. Rev. **78**, 81, 1950. S. Singer, L. K. Neher and R. A. Ruehle, Pulsed photomultipliers for fast scintillation counting, Rev. sci. Instr. **27**, 40-43, 1956 (No. 1).

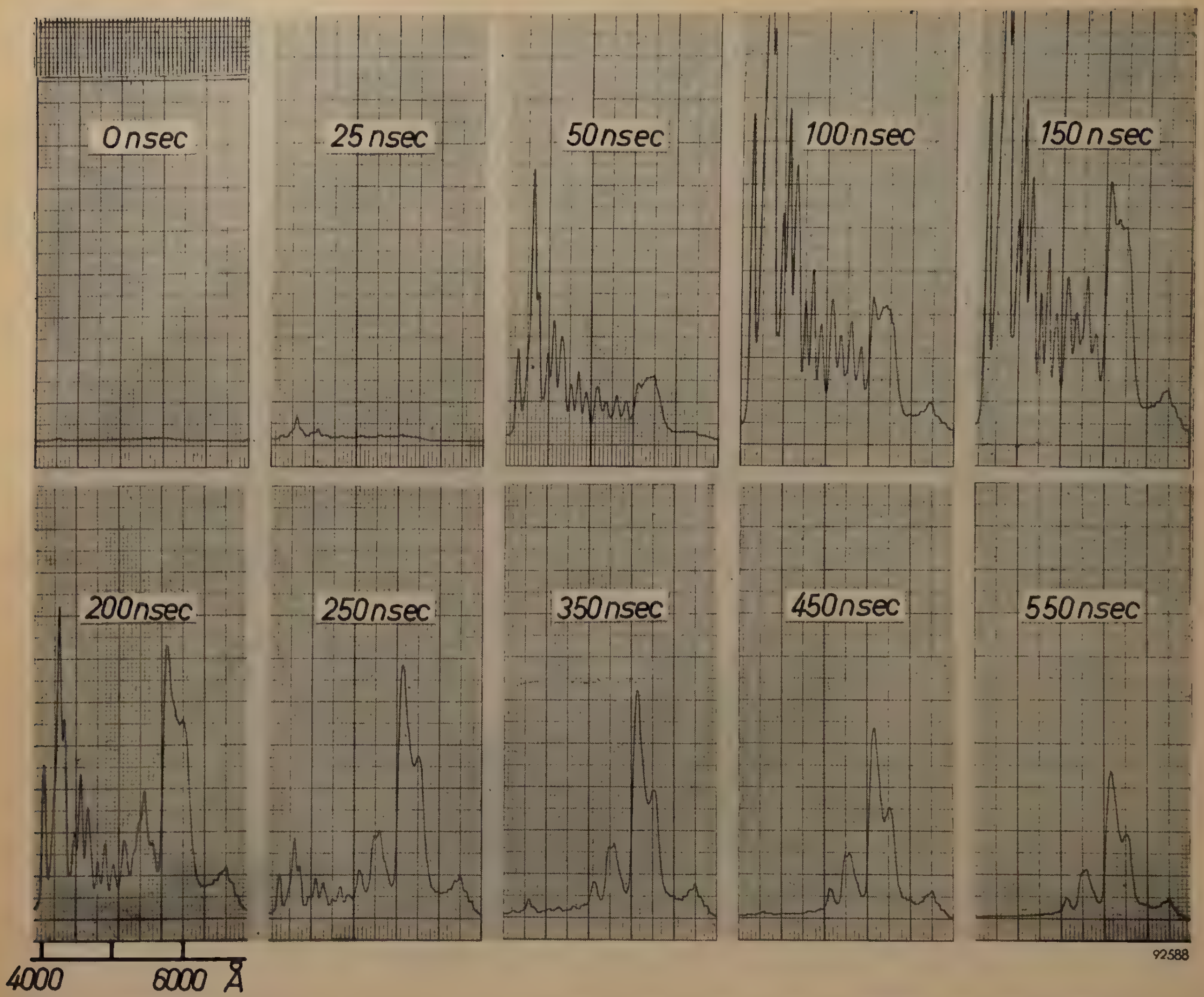

Fig. 6. Time-resolved spectroscopy: a series of spectra obtained from a pulsed nitrogen discharge at successive instants during the pulse, from 0 up to 550 nanoseconds (1 nsec = 10^{-9} sec) after the initiation of the discharge.

The narrow peaks on the left of each spectrum ($\lambda < 5000$ Å) are part of the "2nd Positive" bands of N_2. The broad peaks on the right ($\lambda > 5000$ Å) are groups of unresolved "1st Positive" bands. A sharp cut-off filter, Corning 3389, was used in these runs to eliminate the strong 2nd Positive bands at $\lambda < 4000$ Å, lest their second order spectrum should obscure the much weaker 1st Positive bands. Separate investigation of these bands showed that all 2nd Positive bands had about the same time variation.

Note that the 2nd Pos. bands attain their peak intensity in 100-150 nsec and have practically disappeared at 250 nsec. The 1st Pos. bands appear later (peak in 150-200 nsec) and decay much more slowly. This is explained by the fact that the lower quantum level of the 2nd Pos. bands transition is the upper quantum level for the 1st Pos. bands transition, and this level apparently has a much longer half-life ($\sim 10^{-6}$ sec) than the upper level of the 2nd Pos. bands ($\sim 10^{-7}$ sec) (although other factors may contribute to the long decay time of the 1st Pos. bands, such as absorption from the lower (metastable) level of this transition with subsequent re-emission, or a populating of the (triplet) upper level of this transition from some metastable singlet level as proposed by R. W. Nicholls, J. chem. Phys. **20**, 1040, 1952). Direct experimental data on the half-lives of these levels have not been previously reported.

In similar runs, but under greater spectral dispersion, the individual 1st Pos. bands were resolved. The relative intensities of these bands did not vary greatly during the decay and were approximately equal to those obtained in a normal D.C. glow discharge in nitrogen. This point distinguishes the long decay which we observed ($\sim 10^{-6}$ sec) from the well-known nitrogen afterglow (decay of the order of 1 second), since in the latter case the relative intensities of the bands are entirely different.

when the light is blocked, they do not appear, except for an occasional isolated pip, about one every ten phototube pulses, which permits the conclusion that such "dark pips" are due to thermal electrons emitted at the cathode.

The oscillograms of *fig. 8* will provide an explanation for the higher voltages admissibles under pulsed operation and give an indication of the limits imposed. These pictures were obtained with 3 μsec pulse voltages higher than that used for fig. 1 and with *no light* on the tube. At a voltage little above 2500 V, pips of low amplitude began to appear, at first very erratically and only near the end of the 3 μsec pulse. As the voltage was raised these "noise" pips became more regular, greater in amplitude and number, and appeared earlier in the pulse. The interpretation is that these pips are due to positive ions from residual gas in the tube striking the dynode surfaces and initiating electron avalanches. This gas-generated noise apparently requires several microseconds or even longer to develop at voltages below 2 kV, but less time as the voltage is increased. Even at voltages of 4 kV, however, it is seen that the tube is relatively free of the noise during the first few tenths of a microsecond, as would be expected from calculated transit times of positive ions. It is this delay in the development of gas noise that allows these tubes to be used at very high gains under 10^{-7} sec pulse conditions.

The noise pattern as shown in fig. 8 (obtained for 3 μsec pulses) is unaffected by repetition of the pulses up to rates of at least 1000 per second. Evidently, the tube will recover from the severe gas ionization in less than one millisecond.

Fig. 8 shows the behaviour of the pulsed tube with no light. In actual use, the light falling on the tube will enhance the gas noise breakdown and will evoke the appearance of noise pips at voltages much lower than those used in fig. 8. This may affect the linearity of the relative intensity measurements to some extent. It was found, however, that the magnitude of the noise can be greatly reduced by painting the outside of the photomultiplier tube with finely dispersed graphite and applying to this conducting layer either the cathode pulse voltage or a D.C. voltage equal to its peak. This procedure probably reduces the electric field in the tube and thereby the gas ionization.

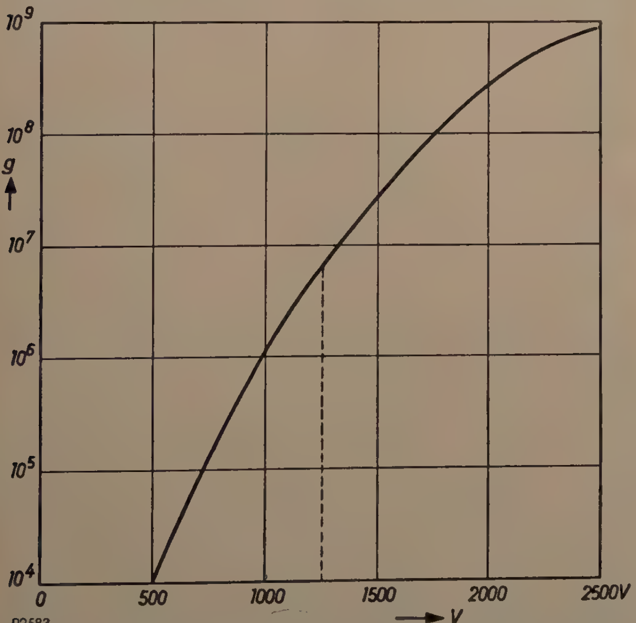

Fig. 7. Gain g obtained when actuating a 1 P 21 photomultiplier tube with a 10^{-7} sec pulse, plotted against the peak voltage applied between cathode and collector.

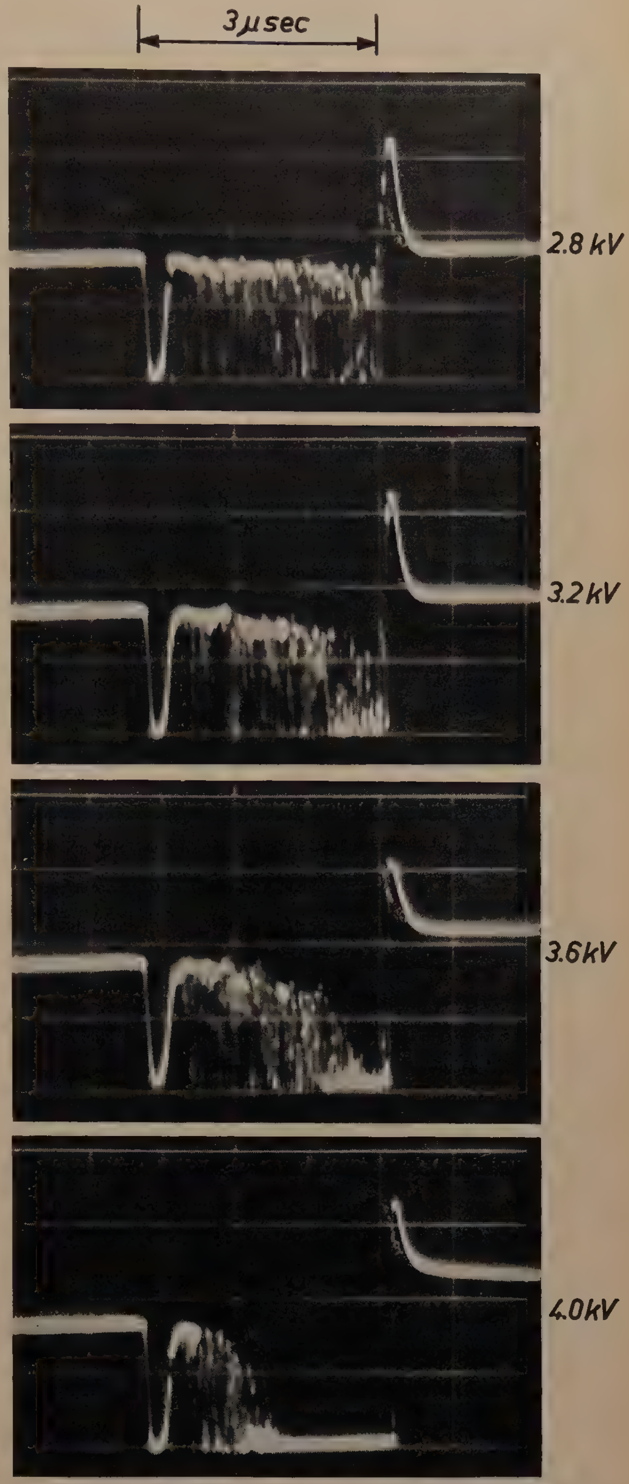

Fig. 8. Oscilloscope traces of the output of a photomultiplier tube during a single 3 μsec pulse, with *no illumination*, at high pulse voltages (peak value indicated at the right). The numerous pips probably are due to positive ions from residual gas in the tube (gas noise). The density of pips at the highest voltages becomes so large towards the end of the pulse as to cause a continuous trace.

It is important to note that a flash of light falling on the pulsed tube in the *beginning* of its "on" time will evoke noise pips continuing during the whole "on" time (after-pulsing). No noise pips appear, however, if the light flash is extinguished *before* the start of the photomultiplier pulse, even if it precedes the latter by as little as 10^{-7} sec. This is

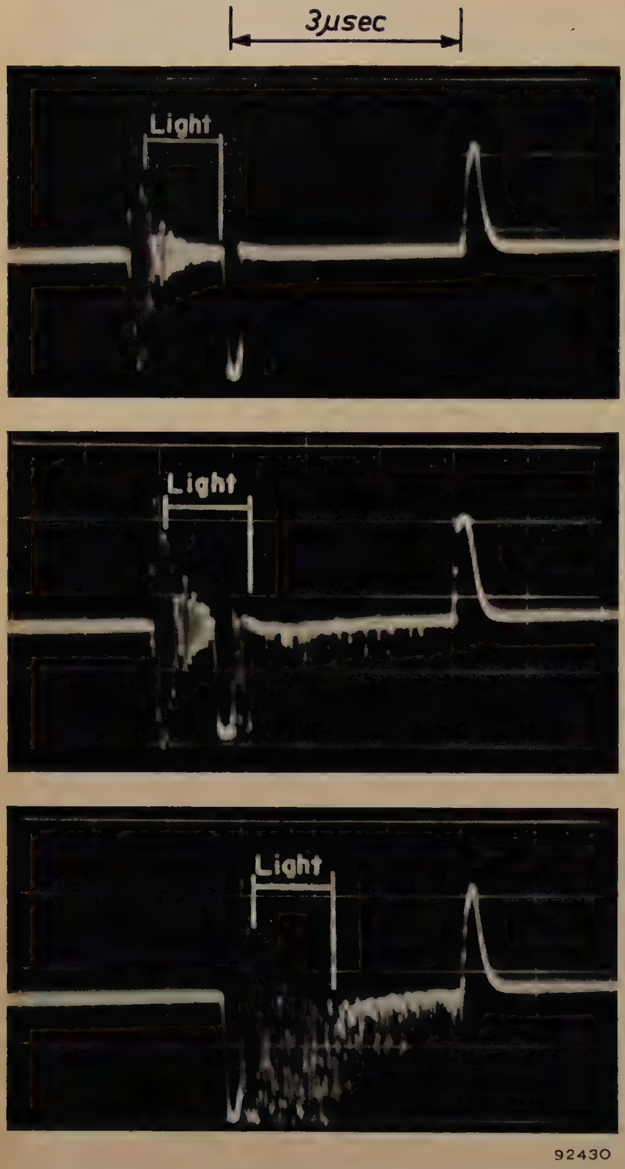

Fig. 9. Same as in fig. 8, at a pulse voltage of 2.0 kV, with a 1 μsec light flash falling on the phototube just prior to or in the beginning of the pulse. No afterpulses whatever are recorded in the first case.

The initiation of the light flash becomes visible in the oscilloscope trace as a damped oscillation picked-up electrically by the oscilloscope from the 20 kV pulse feeding the light source. It is a remarkable fact that the response of the pulsed photomultiplier itself is quite unaffected by such pick-up phenomena. This enables the leading edge of light flashes (build-up phenomena in electrical discharges) to be effectively studied by the stroboscopic method decribed.

demonstrated by the series of oscillograms reproduced in *fig. 9*, showing the signal of a phototube during a 3 μsec pulse, on exposure to a 1 μsec light flash just preceding or overlapping the phototube pulse. Because of this remarkable behaviour of the phototube, the pulsing technique was used in this laboratory in several instances to detect very weak light following an intense light flash, such as in the study of weak afterglows and excitations caused by absorbed light and also in an optical ranging system. In the latter, a bright flash of light is directed at a distant object and the reflected pulse is detected by a pulsed photomultiplier. The weak reflected pulse, received only 0.5 μsec after the initial flash, was detected against the unavoidable local back-scatter which, at the phototube, may be many times greater in intensity. Experiments showed that an intensity ratio of 10^5 between back-scatter and reflected flash was permissible.

A final, not fundamentally but practically important remark concerning the pulsed operation of photomultiplier tubes should be made: the need for light-tight shielding and low level room lighting is much relaxed because of the low duty factor. Further the danger of damage of the tube due to exposure to room light is less because the current is not allowed to assume excessive mean values even with the extremely high gain obtained at high voltages.

Circuits for pulsing the photomultiplier tube

In order to accomplish the required pulsing and phasing, several forms of circuitry have been tried. *Fig. 10* shows one form, using only standard tubes and components. The upper portion of the circuit is for triggering the light source while the lower portion generates the phototube voltage pulse, usually of 10^{-7} sec duration, with peak adjustable from 0 to 5000 V. The common trigger generator *T* of both portions was designed to supply 1-10000 pulses per second. The phase relation between the two output pulses of the circuits is controlled by the potentiometer *Pot* and the step delay line *D*. The duration of the phototube voltage pulse is determined by the length of the coaxial cable *C*, used as a pulse forming network.

For the stroboscopic operation with an "on" time of 10^{-7} sec, it was necessary to make the relative time jitter between the light pulse and the phototube pulse less than 10^{-8} sec. In addition this accuracy had to be maintained when the phase between the two pulses was adjusted over a 5 μsec range. This was the most difficult experimental problem encountered and was accomplished only after careful decoupling, shielding and power supply regulation. Later modification of the circuit incorporated continuously variable time delay networks for the phase control and this greatly reduced the jitter.

The phototube pulse was capacity-coupled to the dynode voltage divider *B*, consisting of ten 100 ohm carbon resistors. This low impedance is required to allow the dynode voltages to rise and fall in times short compared to the 10^{-7} sec pulse duration. It was found that the interelectrode capacitance of the normal 11-pin tube socket of the photomultiplier tube caused too large a pulse round-off. Therefore the voltage divider was connected directly to the base pins of the phototube, as shown in fig. 3. Removing the base of the tube did not give any further improvement.

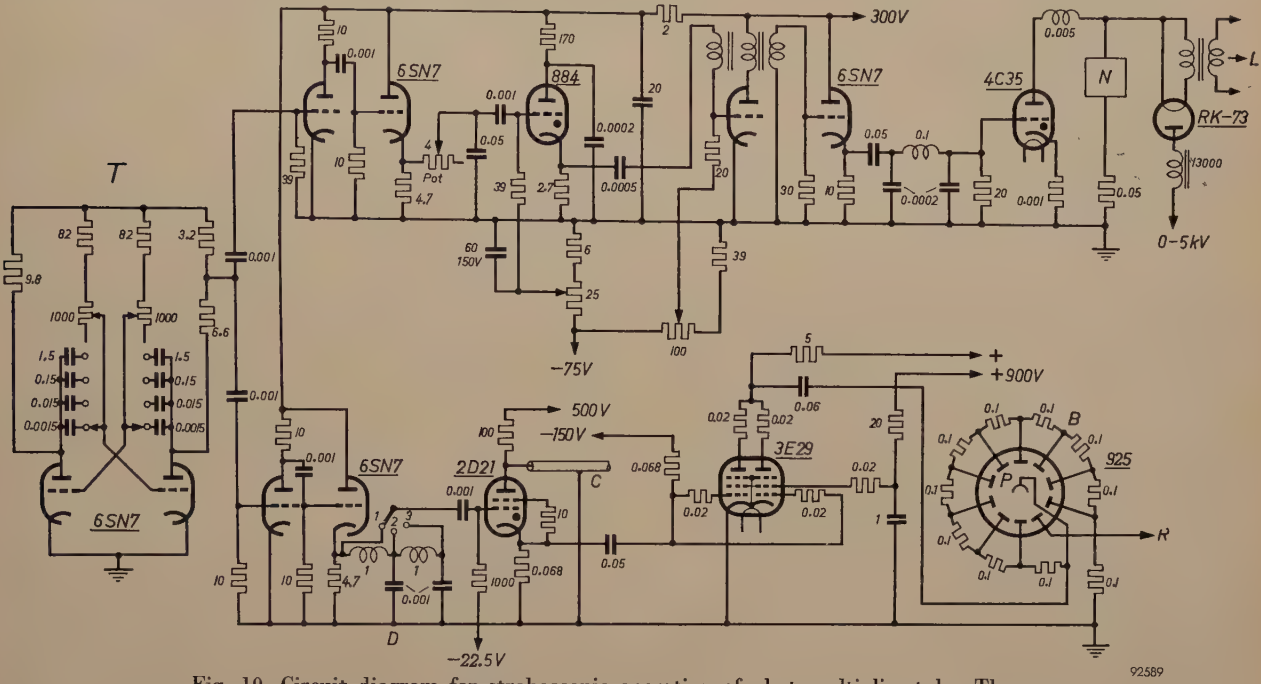

Fig. 10. Circuit diagram for stroboscopic operation of photomultiplier tube. The upper portion produces the pulse fed to the light source (*L*), the lower portion supplies the required voltage pulse (peak 0-5000 V) to the photomultiplier tube *P*. *T* common trigger generator; the potentiometer *Pot* and step delay line *D* control the phasing of light flash and phototube pulse, the coaxial cable *C* determines the duration of the phototube pulse; the pulse-forming network *N* controls the form and duration of the light flash. *B* is the voltage divider for the dynodes. The recording microammeter is connected at *R*.

Several experiments were made in which the voltage applied to only one or two dynodes of the photomultiplier tube was pulsed while the remaining dynodes were maintained at their normal D.C. operating potential. In such an operation one of the dynodes would act as a control grid; the complete cut-off required for the shutter action, however, was not obtained. Some signal was recorded even though the control dynode voltage was allowed to swing several hundred volts in either direction.

The current meter used was a commercial electronic microammeter suitably modified to give full-scale readings at currents down to 10^{-9} amperes, and an output for connection to a 0-10 mV strip chart recorder. Across the input of the meter was placed a suitable capacitor whose capacitance, together with the input impedance of the meter, produced the desired *RC* time constant, for the integration of the signal in successive pulses.

Sensitivity and accuracy of the measurements

It should be realized that according to eq. (1) an average phototube current of 10^{-9} A with a gain $g = 10^9$ and a pulse repetition rate f of say 1000 per sec corresponds to $\bar{n}_p \approx 0.006$, i.e. less than 1 photoelectron per 100 phototube "on" times! Such extremely low intensity signals can be detected and reasonably accurately measured owing to two features of the stroboscopic operation, qualitatively already implied in the description given above: 1) Parasitic current contributions, mainly from thermal electrons, occurring at a rate of about 10^5 per second at 300 °K, are effectively eliminated by the gating action of the phototube: the average number $\bar{n}_t$ of thermal electrons per pulse is about 0.01 (again 1 electron per 100 phototube "on" times). 2) The fluctuations of the measured current are greatly reduced since the rate of the contributing photoelectrons is averaged over a very long *RC* time. The "signal-to-noise ratio" S/N of the phototube collector current is given by the expression [8]):

$$\frac{S}{N} \approx \sqrt{\frac{\overline{g}^2}{\overline{g^2}}\,\frac{\bar{n}_p}{\bar{n}_p+\bar{n}_t}\cdot 2\bar{n}_p fRC}\,, \quad . \; . \; . \quad (2)$$

taking into account the fluctuations of the gain due to random fluctuations in the secondary emission. Assuming a value of 0.75 for $\overline{g}^2/\overline{g^2}$ (determined for a

---

[8]) From an unpublished analysis by F. K. du Pré of this laboratory.

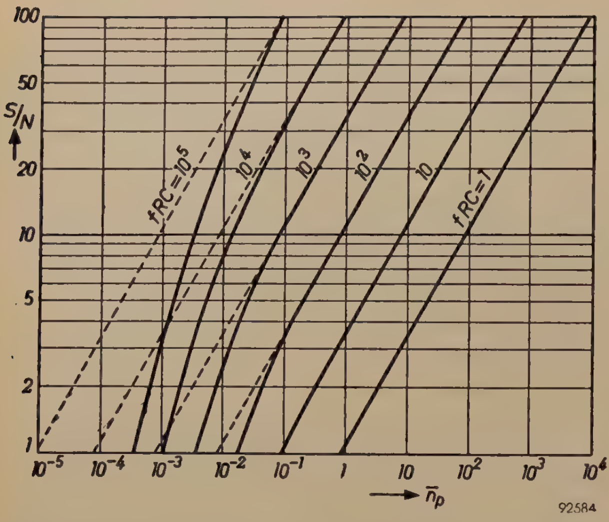

Fig. 11. Signal-to-noise ratio S/N of the photomultiplier-tube collector current, plotted against the average number $\bar{n}_p$ of primary photoelectrons per photomultiplier pulse, for different pulse repetition rates f and integration time constants RC (see eq. 2). The dashed curves would be obtained if no thermal electrons were emitted by the photocathode.

particular RCA 1 P 21 photomultiplier tube by measuring the heights of a large number of pips due to individual electrons in photographs of the type of fig. 1), S/N is plotted against $\bar{n}_p$ in *fig. 11*. It can be seen that a signal-to-noise ratio $S/N = 4$ can be obtained with light flashes producing as little as 1 photoelectron in 1000 flashes, provided the maximum repetition rate $f = 10^4$ per sec and an RC time of 10 seconds are used for the stroboscopic operation.

Since the actual "on" time of the photomultiplier tube is equal to the duration of the dynode voltage pulse minus the total transit time of an electron avalanche through the tube (a few 10^{-8} sec), the *spread* in the transit time, which may amount to a few 10^{-9} sec, will be fully felt in the "on" time and will therefore ultimately limit the time resolution of which the stroboscopic scanning method is capable. A practical limit on the resolution is imposed by the jitter caused by the circuitry as mentioned above. In fig. 4 the resolution obtained in scanning a periodic 1 μsec light flash by means of 10^{-7} sec phototube pulses is seen to be better than 3×10^{-8} sec (half-value width of the first Hα-peak in fig. 4*a*).

Summary. The time variation of the light intensity in weak light flashes can be analyzed by using a photomultiplier tube supplied with pulsed dynode voltages. The pulsed tube acts as an effective light shutter, providing an "on" time as short as 10^{-7} sec if desired. By periodic repetition of the light flash and synchronization with the photomultiplier tube pulses in a constant phase relation, separate instants of the light flash can be isolated and the instantaneous intensity accurately measured by integrating the phototube collector current over a long period. Circuits are described which permit repetition rates up to 10 000 per sec and integration periods of 10 sec or even longer. The 10^{-7} sec phototube pulse can be phased through the complete light flash (of say 10^{-6} sec duration), providing a stroboscopic analysis of the flash. The dynode voltages in the pulsed operation of the phototube can be raised considerably above those admissible in normal D.C. operation, resulting in a much higher gain (up to 10^9) and permitting the measurement of extremely low light intensities, e.g. in narrow spectral regions of the total light emitted. Examples of "time-resolved spectograms" obtained by this method are presented in this article and some details concerning the pulsed operation of the photo-multiplier tube and the accuracy of the measurements are discussed. The signal-to-noise ratio can be high even with signals producing a fraction of one photoelectron per pulse, since the gating action of the pulsed phototube effectively suppresses thermionic and other noise current contributions. The time resolution can be made better than 3×10^{-8} sec by effectively reducing the time jitter between light pulses and phototube pulses.

APPLICATIONS OF THE INTERFERENCE OF LIGHT IN THIN FILMS

by P. M. van ALPHEN.

535.417:621.397.2

The phenomenon of the interference of light in thin films has been put to use for some time in optical instruments, e.g. prismatic binoculars, and in recent years also in colour television. In view of some articles on the latter subject, which are to appear shortly in this Review, the article below gives a short discussion of the theory and of the various applications of interference at thin films.

Probably everyone, as a child, has been fascinated by the phenomenon of optical interference: the multi-coloured patch of oil on wet asphalt and the beautiful colours of a soap bubble in the sun will be familiar to everybody. Centuries ago these colours provoked curiosity; Newton and many others investigated these phenomena.

For many years now, interest in this interference phenomenon has outgrown its purely scientific aspects: it is also of practical value. We shall discuss here some aspects of this technical development, thereby, it may be, illuminating the fascination of a soap bubble.

Optical interference in a thin transparent film

When light is reflected from a thin transparent film, interference occurs and, as a result, certain colour effects can be observed. To make this clear, let us consider *fig. 1*, in which *1* represents a very thin film of water spread over a glass plate *2*. If a beam of white light falls almost perpendicularly on it, some portion of the light will be reflected from each of the two boundary surfaces, *a* and *b*. The reflected rays are parallel ($AR // CS$). Since the light reflected at B has travelled a longer path than that reflected at A, and since both rays originate from the same source, a phase difference occurs between the two waves and interference can take place. If the phase difference corresponds to a whole number of wavelengths, the waves reinforce each other and the intensity of the reflected light is increased; if the phase difference represents an odd number of half wavelengths, then the waves oppose one another and the intensity of the reflected light is decreased, perhaps to zero. In the first case we have a *high-reflection* film, in the second, a *low-reflection* film. Since the phenomena are dependent on the wavelength, increased reflection for one colour can coincide with decreased reflection for another.

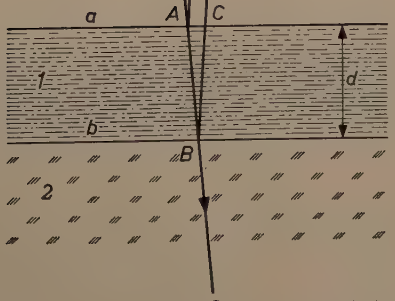

Fig. 1. Reflection, for almost normal incidence, of ray *PA* (in air, medium *0*) at a film of water (medium *1*) on glass (medium *2*). *PABQ* and *BCS* are assumed to be straight lines.

The magnitude of the phase difference is easily found. For normal incidence the path difference is twice the thickness of the film d. The wavelength of light in water is λ/n, where λ is the wavelength of light in air and n the refractive index of water. The phase difference in this case is thus $(2nd/\lambda)\times 2\pi$ radians. If the rays do not strike at right angles, but at an angle α to the normal to the film (*fig. 2*), the phase difference becomes:

$$\frac{2nd\ \cos\vartheta}{\lambda}\times 2\pi \text{ radians}, \quad . \ . \ . \ . \quad (1)$$

where ϑ is the angle which the refracted ray AB makes with the normal ($\sin\alpha/\sin\vartheta = n$).

Since the path in water ABC is equal to $2d/\cos\vartheta$, one might suppose that in equation (1) the factor $\cos\vartheta$ should be in the denominator. Therefore we give here in brief the derivation of (1).

The "optical path" of the ray ABC in water of refractive index n is $2nd/\cos\vartheta$. The light reflected at A must travel a distance AC' before it reaches the wave front of C. Now $AC' = AC\sin\alpha$, $AC = 2d\tan\vartheta$ and $\sin\alpha/\sin\vartheta = n$, thus

$$AC' = 2d\tan\vartheta\sin\alpha = 2nd\,\frac{\sin^2\vartheta}{\cos\vartheta}.$$

The optical path difference is therefore:

$$2nd\left(\frac{1}{\cos\vartheta}-\frac{\sin^2\vartheta}{\cos\vartheta}\right)=2nd\cos\vartheta,$$

as stated in (1).

The phase difference is thus less for obliquely incident rays than for those with normal incidence.

Besides this phase difference, there is sometimes a phase jump as well, in cases where the reflection takes place at an optically denser medium, analagous to the phase jump occurring at the end of vibrating strings, organ pipes, Lecher lines, waveguides, etc.

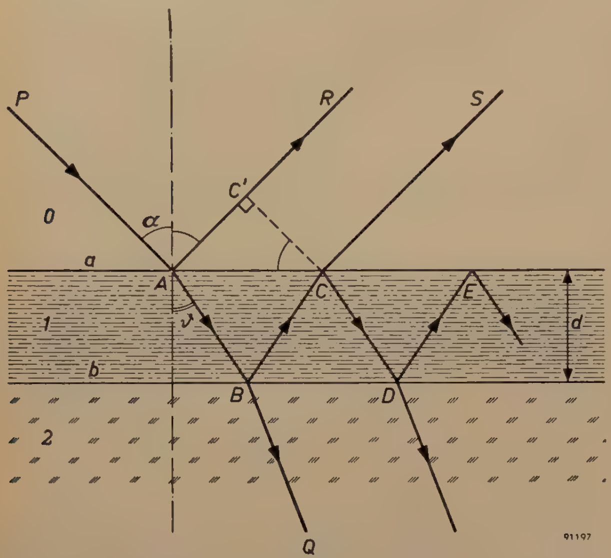

Fig. 2. As in fig. 1 but now for oblique incidence. Some of the multiple reflections are shown.

For normal incidence, the phase jump is π radians. In the example shown in fig. 1, both reflections take place at optically denser media (water is denser than air, glass denser than water). Both at A and at B, for normal incidence, a phase jump of π radians occurs, so that the phase difference is not affected. However, if one is dealing with a free film, such as a soap bubble, or if layer *1* in fig. 1 is of a material which is optically denser than glass, then only the first reflection takes place at an optically denser medium, while the second occurs at an optically less dense medium and no phase jump occurs for the latter. For normal incidence the condition for maximum reflection is then:

$$\frac{2nd}{\lambda}+\tfrac{1}{2}=k, \quad \ldots\ldots \quad (2a)$$

and that for minimum reflected light:

$$\frac{2nd}{\lambda}+\tfrac{1}{2}=k+\tfrac{1}{2}, \quad \ldots\ldots \quad (2b)$$

where k is an integer.

Reflection coefficient of a boundary surface and of a layer.

Let us now consider the reflection coefficient r, for the case of a ray travelling in one medium (e.g. air) and being reflected at the boundary surface of a denser medium (e.g. glass). r is dependent on the refractive index n from the one medium to the other, the angle of incidence and the direction of polarisation, and is given by the formulae of Fresnel. At normal incidence these formulae reduce to

$$r=\left(\frac{n-1}{n+1}\right)^2. \quad \ldots\ldots \quad (3)$$

For air-glass ($n=1.5$) we find: $r=0.04$, and for air-zinc sulphide ($n=2.4$): $r=0.17$.

Equation (3) can easily be deduced from the fact that according to Maxwell's theory the tangential components of both the electrical field strength $\boldsymbol{E}$ and the magnetic field strength $\boldsymbol{H}$ at the boundary between two media are equal (*fig. 3*):

$$\left.\begin{array}{l} E_1-E_1'=E_2,\\ H_1+H_1'=H_2, \end{array}\right\}, \quad \ldots\ldots \quad (4)$$

there being no other components for normal incidence. (Suffix 1 refers to one medium, suffix 2 to the other and the accent to the reflected ray. There is a negative sign in one equation and a positive sign in the other because the incident and reflected rays move in opposite directions: thus one of the vectors, e.g. the $\boldsymbol{E}$-vector, is reversed in direction.)

Now $H_1=\sqrt{\varepsilon_1}E_1$, $H_1'=\sqrt{\varepsilon_1}E_1'$, $H_2=\sqrt{\varepsilon_2}E_2$ and $n=\sqrt{\varepsilon_2/\varepsilon_1}$ (ε_1 and ε_2 are the dielectric constants), so that instead of (4) we can write:

$$E_1-E_1'=E_2,$$
$$E_1+E_1'=nE_2.$$

By subtraction and addition we obtain:

$$E_1'=\tfrac{1}{2}(n-1)E_2,$$
$$E_1\ =\tfrac{1}{2}(n+1)E_2,$$

thus

$$\frac{E_1'}{E_1}=\frac{n-1}{n+1}.$$

The reflection coefficient r is the square of this amplitude ratio, thus

$$r=\left(\frac{n-1}{n+1}\right)^2. \quad \ldots\ldots \quad (3)$$

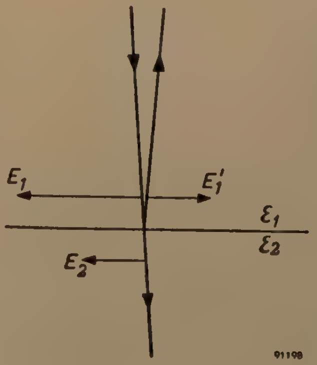

Fig. 3. The almost normally incident ray and the reflected and the refracted rays at the boundary of two media of dielectric constants ε_1 and ε_2. The tangential components of the electric field are E_1, E_1' and E_2 respectively. The tangential components of the magnetic field are perpendicular to the plane of the drawing and all point in the same direction.

If we are dealing not with one boundary surface, but with two (or more), as in the case of the water layer (fig. 2) or a soap film, then for accurate results, account must be taken of repeated reflections: only a portion (*CS*) of the ray *BC* in fig. 2 leaves the film, while the remainder is reflected as *CD*; of this a further portion is reflected as *DE*, and so on. At all these reflections a phase jump may or may not take place, according as the refractive index of the film is smaller or larger than that of the adjoining medium. Taking all this into account, we find for the reflection coefficient *R* of the layer:

$$R = \frac{\varrho_a^2 + 2\varrho_a\varrho_b \cos 2\delta + \varrho_b^2}{1 + 2\varrho_a \varrho_b \cos 2\delta + \varrho_a^2 \varrho_b^2} . \quad . \quad . \quad (5)$$

In this expression

$$\delta = \frac{2\pi}{\lambda} n_1 d \cos \vartheta , \quad . \quad . \quad . \quad . \quad (6)$$

and ϱ_a^2 and ϱ_b^2 are the Fresnel reflection coefficients at the boundary surfaces *a* and *b* respectively. For normal incidence ϱ_a and ϱ_b take the simple form:

$$\varrho_a = \frac{n_0 - n_1}{n_0 + n_1} , \qquad \varrho_b = \frac{n_1 - n_2}{n_1 + n_2} .$$

n_0, n_1 and n_2 are the refractive indices (with respect to vacuum, or air) of the media *0* 1), *1* and *2*. Whether or not a phase shift occurs depends on the sign of ϱ_a and ϱ_b.

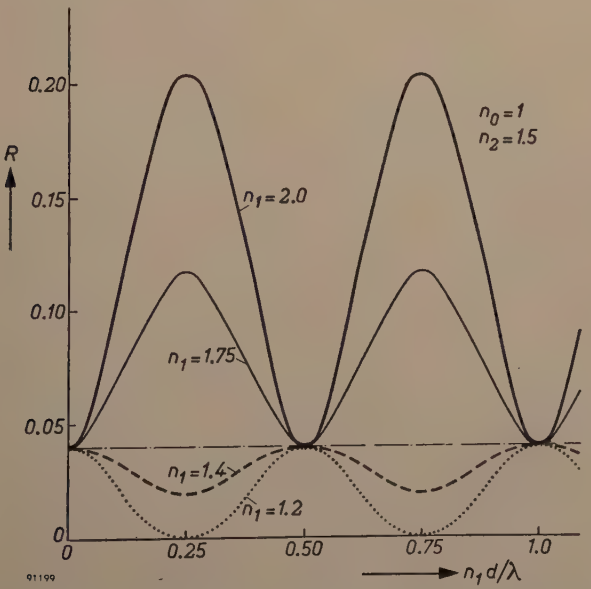

Fig. 4. Reflection coefficient *R* of a thin film (thickness *d*, refractive index n_1) as function of $n_1 d/\lambda$, for various values of n_1. The refractive indices n_0 and n_2 of the adjacent media are 1 and 1.5 respectively.

Substituting the expressions for ϱ_a and ϱ_b in (5), we find for *R* at normal incidence:

$$R = \frac{(n_0^2+n_1^2)(n_1^2+n_2^2) - 4n_0n_1^2n_2 + (n_0^2-n_1^2)(n_1^2-n_2^2)\cos 2\delta}{(n_0^2+n_1^2)(n_1^2+n_2^2) + 4n_0n_1^2n_2 + (n_0^2-n_1^2)(n_1^2-n_2^2)\cos 2\delta} . \quad (7)$$

The thickness of the film *d* and the wavelength λ occur as d/λ in the angle δ, see (6); the fact that the refractive indices depend to some extent on λ (dispersion) has been neglected.

Fig. 4 shows *R* as a function of $n_1 d/\lambda$ drawn for several values of n_1, with $n_0 = 1$ (air) and $n_2 = 1.5$ (glass). The full lines ($n_1 > n_2$, no phase jump at boundary *b*) show high reflection, the broken and dotted lines ($n_1 < n_2$, phase shift at the boundary) show low reflection. Extreme values of *R* occur when $n_1 d = (2k+1)\lambda/4$ and when $n_1 d = 2k\lambda/4$. The magnitude of the extreme value and its nature (maximum or minimum) are given below:

Extreme value of *R*	$n_2 > n_1 > n_0$ (broken lines fig. 4)	$n_2 < n_1 > n_0$ (full lines fig. 4)
$\left(\frac{n_1^2 - n_0 n_2}{n_1^2 + n_0 n_2}\right)^2$	minimum at $n_1 d = (2k+1)\lambda/4$	maximum at $n_1 d = (2k+1)\lambda/4$
$\left(\frac{n_2 - n_0}{n_2 + n_0}\right)^2$	maximum at $n_1 d = 2k\lambda/4$	minimum at $n_1 d = 2k\lambda/4$

Low-reflection films

From the table above can be seen that the minima in the broken curves become zero if $n_1 = \sqrt{n_0 n_2}$ (i.e. if $n_1 = \sqrt{n_2}$ when medium *0* is air), and the minima occur at a film thickness $d = \frac{1}{4}\lambda/n_1$, $\frac{3}{4}\lambda/n_1$, and so on. The reflection from a glass surface could thus be reduced by the application of a film of a material for which $n_1 = \sqrt{1.5} = 1.23$, so reducing the loss of light by reflection in optical instruments. Materials with such a small refractive index, however, are unknown. In practice, one uses materials with the smallest possible refractive index, such as $NaAlF_4$ (cryolite) for which $n_1 = 1.35$, or MgF_2 for which $n_1 = 1.38$, applying them in such a porous form that the effective refractive index is about 1.30. The reflection which, for untreated glass, is 4.2%, is then reduced to 0.25% for the wavelength λ for which $n_1 d = \frac{1}{4}\lambda$. For light of wavelength $\lambda' = \frac{1}{2}\lambda$ the reflection is of course a maximum, but its magnitude is $(n_2 - 1)^2/(n_2 + 1)^2$, which is the value for reflection from the untreated glass surface; in other words, the layer does not increase the reflection for any wavelength (see

---

1) By putting $n_0 = 1$ in the expression for ϱ_a, we find for ϱ_a^2 the same as equation (3), where the medium *0* was assumed to be air.

fig. 4). The thickness of the film is usually chosen so that the reflection reduction occurs in the region of the green; the glass then still reflects some red and blue, which gives it a violet appearance. An important point is that the layer absorbs very little. In instruments with many glass surfaces, e.g. prismatic binoculars and multi-component lenses, this reduction of the reflection can considerably improve the contrast.

By applying two or three films of different materials to the glass, the reflection can be brought to a minimum for two or three different wavelengths and so greatly reduced over the whole visible range. The effect is then rather strongly dependent on the angle of incidence. If the thicknesses of the films are chosen for normal incidence, then the path differences will be smaller for other angles of incidence (factor cos ϑ in (1)) — in varying degree in the different layers — which will reduce the effect.

High-reflection films

A high-reflection film can be of use, for example, to improve the reflection from a metal mirror. By coating aluminium (reflection coefficient 89%) with a $\frac{1}{4}\lambda$-film of SiO and a $\frac{1}{4}\lambda$-film of TiO_2, it is possible to give it a reflection coefficient of 95%.

Even more interesting is its use for semi-reflecting mirrors, which show negligibly small absorption. A semi-reflecting mirror in the form of a thin transparent film of metal always produces considerable absorption; silver, for instance, reflects 30%, transmits 30% and absorbs 40%. If we apply to glass a material for which $n_1 = 2.7$, then according to the first formula in the table above, the maximum of R is equal to 43%; owing to the negligible absorption, the transmission is thus 57%. In this way one obtains a semi-reflecting mirror which is practically free from losses. TiO_2, Sb_2S_3 and ZnS are suitable for use as the material for the film. If, instead of applying the film directly to the glass, an intermediate layer of thickness $\frac{1}{4}\lambda/n_2$ and smaller refractive index are used, the reflection can be increased to 52%.

Colour-separating (dichroic) mirrors

Up to now, we have mainly been concerned with light of a constant wavelength λ. We shall now consider what happens when λ is variable and the film thickness d constant. If we once more neglect dispersion, we can read off the reflection coefficient R of a film as a function of λ^{-1} from fig. 4. We see that in the case where $n_2 < n_1 > n_0$, light of wavelengths $\lambda_{\max} = 4n_1d/(2k+1)$ suffers maximum reflection and light of wavelengths $\lambda_{\min} = 4n_1d/2k$ minimum reflection, i.e. maximum transmission. Partial separation of the colours thus occurs.

This effect can be enhanced in the same way that the purification of materials by distillation or recrystallisation can be improved, namely by repeating the process, in this case by allowing the light to pass through another thin layer. For this purpose a number of thin layers of high refractive index must be applied one after the other. It is clear that these layers must remain separate from each other, or the necessary boundary surfaces would disappear and one would obtain a single thick layer. The separation is achieved by means of a material of low refractive index. The technique of applying such films will be dealt with presently.

There is, however, one more condition which must be fulfilled. The rays transmitted and reflected by the various layers will exhibit relative phase differences; in combining a number of layers, therefore, one must ensure that the maximum from one layer reinforces that from the following layer and does not cancel it. The layers must thus lie at a very definite distance from one another, that is to say, the separating layers of low refractive index must be of sufficient thickness. The separating layers are usually composed of alkali fluorides which, like the other layers, are applied by evaporation. These are essentially the same materials as are suitable for low-reflection films.

Since corresponding points on the reflecting layers must lie at an optical distance of $\frac{1}{2}\lambda$ (i.e. an actual distance of $\frac{1}{2}\lambda/n_1$) apart — the phase difference must be 2π, but the distance is travelled twice — and the layer itself has an optical thickness of $\frac{1}{4}\lambda$, the intermediate layers should also produce an optical separation of $\frac{1}{4}\lambda$. One arrives thus at a pile of layers of alternating high and low refractive index, all with an optical thickness of $\frac{1}{4}\lambda$.

By this combination of a number of layers the reflection as function of λ^{-1} takes on another form: the curve becomes steeper and secondary maxima appear in increasing numbers as the number of layers is increased. The steepness of the curve is easily understood when one remembers that with, say, seven layers even the first and last surfaces must still work together; small deviations in d or λ are additive and are more likely to produce appreciable phase differences when more layers are involved. By not making the layers all of exactly the same thickness, the secondary maxima can be weakened without much effect on the principal maximum.

The problem of calculating the interference in a multiple layer has much in common with that in the optical grating where the light passes through a number of narrow slits placed close to each other. The multiple layer is a sort of "plane grating". The mathematical treatment is more difficult than that of the slit grating, in the first place because account must be taken of repeated reflections between the layers, and further because the intensity of the light falling on a given layer is different from that on the preceding layer, since a portion is reflected at each layer. Various methods, partially graphic, are known by which the theoretical curve can be calculated. *Fig. 5* shows the results of a calculation for a single layer of zinc sulphide and for three, five and seven layers, alternated with cryolite, with glass as the carrier. Experimentally determined curves generally differ from those calculated because the layers are not sufficiently homogeneous and not everywhere of exactly the same thickness, and because dispersion has been neglected. *Fig. 6* shows two measured curves relating to dichroic mirrors made in this laboratory.

Preparation

Before discussing the applications of dichroic mirrors, we shall say something about their preparation.

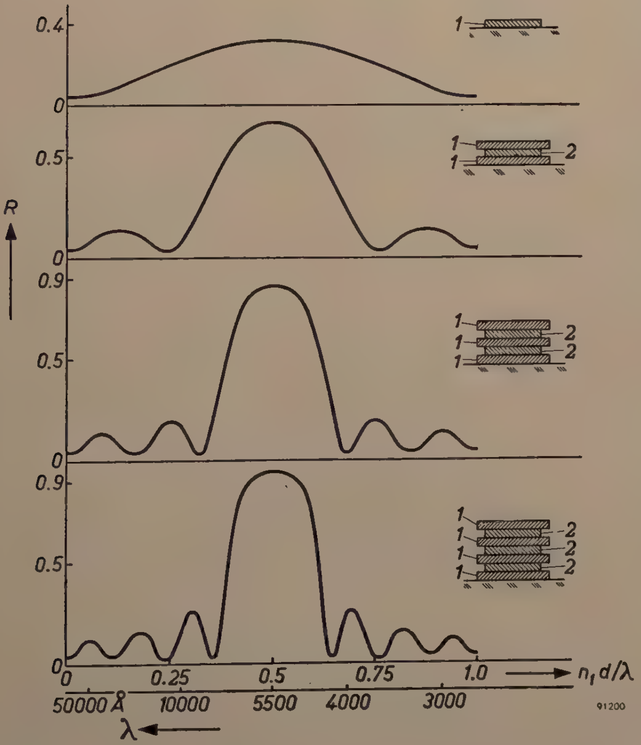

Fig. 5. Reflection coefficient R (calculated) for a single layer of zinc sulphide and for three-, five- and seven-fold layers on glass. The multiple layers consist of alternate layers of zinc sulphide *1* (thickness d, refractive index 2.4) and cryolite *2* (refractive index 1.3); the carrier substance is glass (refractive index 1.5).

As was shown above, one requires layers of optical thickness $\frac{1}{4}\lambda$ or an odd multiple of this quantity, thus of the order of 10^{-4} mm. Apart from mechanical methods such as rolling (various metals), beating (gold) and blowing (glass, soap bubbles), other methods were known of old by which thin films could be produced, such as etching, oxidizing and "burning" (platinum). In the last decades the development of vacuum technique has stimulated sublimation methods, by which the material to be applied is produced in vapour form by cathode atomization or evaporation in high vacuum and deposited from the gas phase in solid form on the material to be coated. Particularly the evaporation method is much used. Not only metals, but also many salts can be applied in this way. This process is conditional on the material not decomposing below about 1500 °C and having a reasonable vapour pressure.

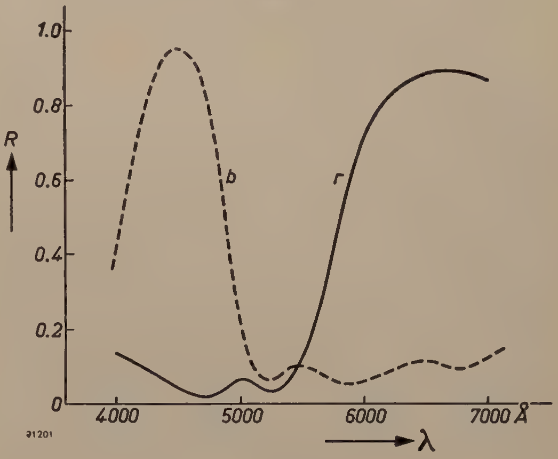

Fig. 6. Measured reflection coefficient R of two dichroic mirrors as function of the wavelength; r for a red, b for a blue reflecting mirror.

Our installation (*fig.* 7) is fitted up as follows. A dome K (*fig. 8*) rests on a table T and is sealed by a rubber ring R which is vacuum-tight when the dome is pumped out. Passing through the table around the pump tube a number of rigid molybdenum current leads I are mounted; these are electrically insulated from the table by a ceramic material and are capable of carrying 300 A. Evaporation elements V can be fixed to the conducting rods. The glass plate G to be coated rests on three rods S; two of these rods have a cap B at the top which can freely rotate and on the third rod this cap is fixed but the rod itself can be turned by a motor, for which purpose it passes through the table via a vacuum-tight bush L. When the motor is working, the glass plate rotates so that it can be coated very uniformly.

The evaporation elements *V* may consists of a crucible, heated by a tungsten spiral or a strip of tungsten or molybdenum. In many cases we use a type which is rather similar to an indirectly heated cathode. Hollows are turned in both top and bottom of a cylindrical piece of molybdenum (*fig. 9*). A tungsten heating coil, insulated with aluminium oxide is mounted in the lower cavity; the upper cavity, which serves as the crucible, contains the material to be evaporated. When the molybdenum is heated, the material evaporates and is deposited on the glass plate. In our apparatus twelve of these evaporation elements can be introduced and they can be heated independently. It is thus possible to deposit twelve successive layers without opening the dome. Also mounted under the dome are a lamp and a photo-cell by means of which the transmission of the plate can be measured during the sublimation process; part of a strip-chart recording of such a measurement can be seen in fig. 7.

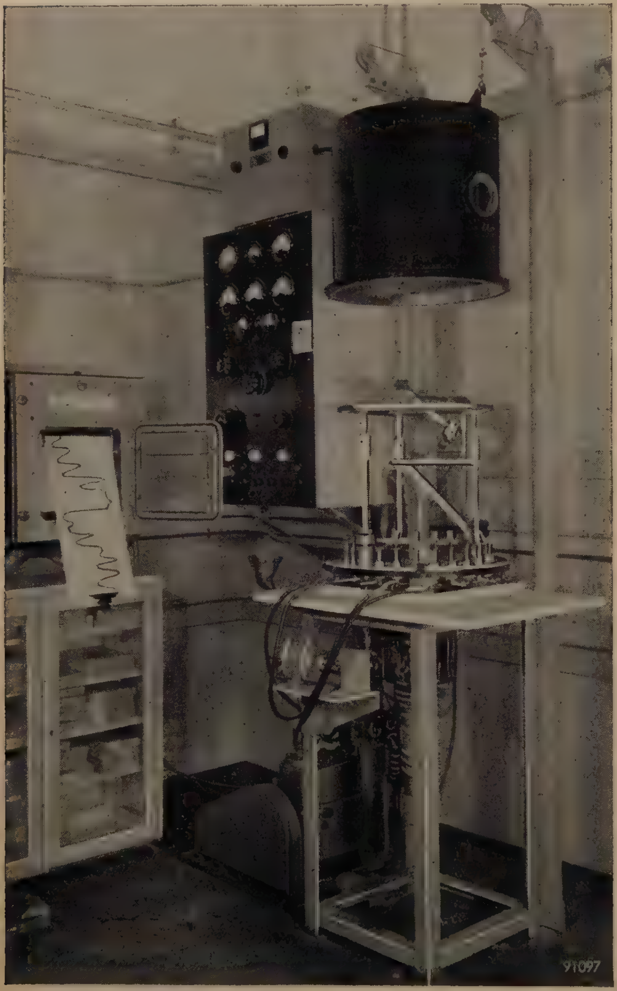

Fig. 7. Equipment for the sublimation of thin films in vacuum. The dome under which the sublimation is carried out (compare fig. 8) is shown raised; in the centre background is the switchboard for the control of the heating current to the evaporation elements. On the left can be seen a recording potentiometer which records the transmission of the glass plate under treatment as a function of the time.

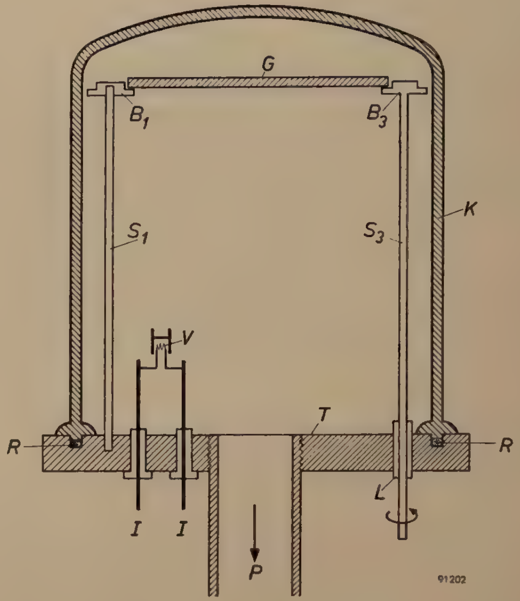

Fig. 8. Apparatus for sublimation of thin films. *G* is the glass plate being coated, *K* the dome, sealed vacuum-tight to the table *T* by the rubber ring *R*, *P* the exhaust tube, *V* one of the evaporation elements, with heater current leads *I*. S_1 fixed supporting rod with free cap B_1 (S_2, B_2 idem, not shown). S_3 rotating rod with fixed cap B_3, mounted in vacuum-tight seal *L* which leads it through the table; this rod is driven by a motor and causes plate *G* to rotate slowly.

The dome is suspended by steel cables passing over pulleys to counterweights. When air has been allowed to enter, the dome can thus easily be lifted up and the evaporation space is then accessible from every side.

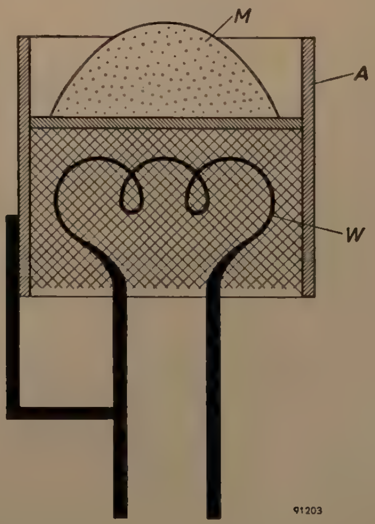

Fig. 9. Section of evaporation element. *A* molybdenum cup, *W* tungsten heater coil (insulated with aluminium oxide). *M* is the substance to be evaporated.

Applications of colour-separating mirrors

As will shortly be described in more detail in this Review, a colour-television picture can be obtained by superimposing three pictures, one in each of three basic colours (e.g. red, green and blue). One difficulty involved is that the three monochromatic pictures must be exactly equal in shape and size. Now if three projector tubes are placed beside one another in front of a screen (*fig. 10*), the middle one will throw a rectangular picture on the screen, while the other two give trapezium-shaped pictures which deviate in opposite directions from the rectangle. There is no simple way in which to correct this fault by normal optical means in high aperture systems without losing a great deal in definition.

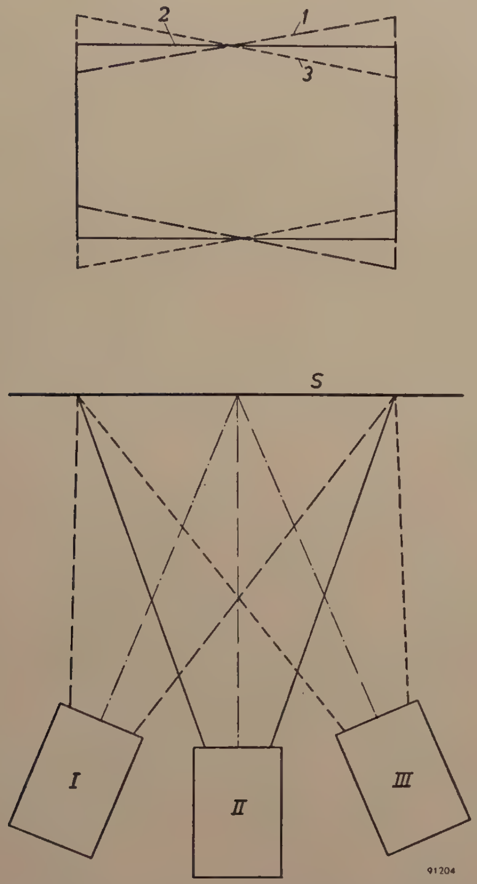

Fig. 10. The pictures from the three projectors *I*, *II* and *III* on the screen *S* do not properly coincide, since the projectors *I* and *III*, placed at an angle, give trapezium-shaped pictures (*1* and *3*), and the projector *II* a rectangular picture (*2*).

It is therefore preferable to project the pictures effectively from the same point. This can be achieved with the help of semi-reflecting mirrors (*fig. 11*). With normal semi-reflecting metal mirrors however, the loss of light would be very great. As already stated above, such mirrors reflect and transmit about 30%. About 30% of the light from projector *R* thus reaches the screen by reflection from mirror *r*, but only about 9% of the light from *G* and *B* is usefully employed. This lowers the intensity of the picture, so that bright colours are difficult to achieve. The result is better, but still unsatisfactory, when the mirrors are coated with SiO-TiO_2 (25% useful light instead of 9%).

Dichroic mirrors of the type discussed above, give a considerably more efficient use of the light. It can be seen from fig. 6 that the mirror *r* in fig. 11 reflects 88% of the red light from projector *R*, mirror *b* 93% of the blue light from projector *B*. Of this blue light only 6% is lost by reflection from mirror *r*, so that 87% reaches the screen. The green light from projector *G* loses 10% at mirror *b* and 10% at mirror *r* by reflection, so that 81% is still effective.

In the arrangement in fig. 11, the mirror *r* is much larger than mirror *b*. This is necessary because *r* is situated much further from the projectors *G* and *B* and the beam therefore has a larger cross-section at *r* than at *b*. In order to make *r* smaller, preference is often given to an arrangement by which the mirrors cut one another, forming a cross (*fig. 12*). Here use is made of the fact that not only does blue light suffer little loss in passing through a red-reflecting mirror, but also that red will pass through a blue-reflecting mirror without much loss (see fig. 6). The green light in fig. 12, as in fig. 11, passes through both mirrors.

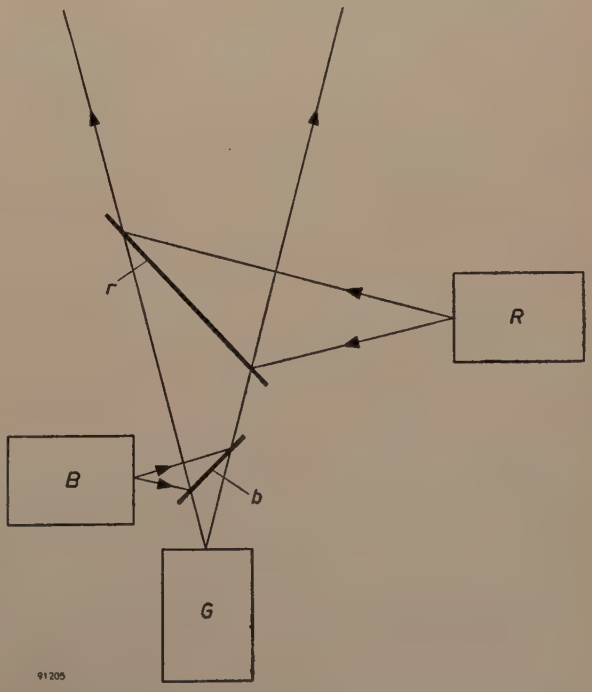

Fig. 11. With the use of semi-reflecting, dichroic mirrors, the beams from the three projectors (*R* red, *G* green, *B* blue) can be made to coincide, with little loss of light. *r* is a red, *b* a blue reflecting mirror.

In the last example, light from three monochromatic sources was combined to give one coloured picture. The reverse can also be done, that is, the light from a multi-coloured object can be split into three basic colours by means of a similar combination of mirrors. This is done in some colour television cameras. Apart from the more efficient use of the available light, another important point is that the scene is viewed from one place, not three, and in all colours at the same instant.

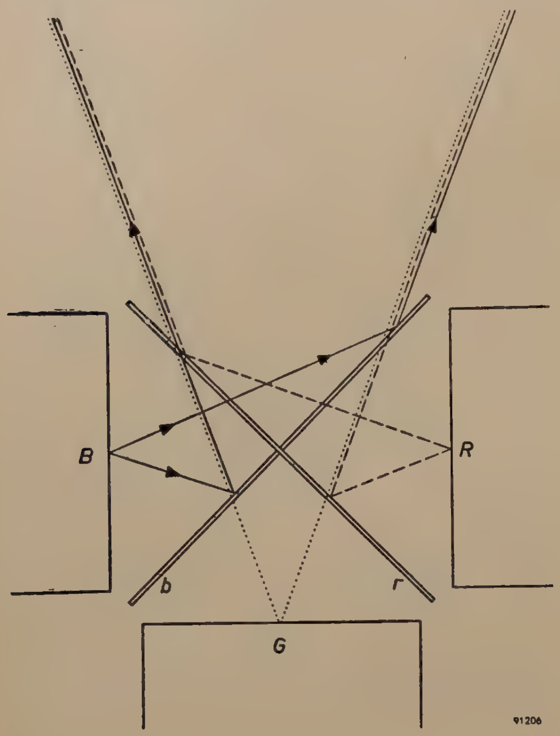

Fig. 12. As fig. 11, but with the arrangement modified so that the red reflecting mirror *r* need be no larger than the blue reflecting mirror *b*.

Corrective measures

Since the mirror must be accurately plane, the glass plate which carries the interference layers must be fairly thick. This thickness makes certain corrections necessary.

In the first place, the thickness prevents light reflected from the back surface from coinciding with that reflected from the front surface, so that double images occur. The image originating from the back surface is of the complementary colour and is not very weak, since it is of the colour which is transmitted strongly by the interference layer. This disturbing reflection can be weakened by providing the back of the mirror with a film with low-reflection properties for the colour of the transmitted light.

In the second place, the thickness of a plane-parallel glass plate placed at an angle in a non-parallel (thus convergent or divergent) beam of light, gives rise to optical aberrations. In *fig. 13* we see how ray *1* is but slightly displaced sideways by the plate while ray *3* is displaced to a much greater degree. This causes asymmetric focusing at the image point *B*. Rays obtained by rotating ray *1* about the normal *LM* (*M* is the point where the incident rays, if produced, intersect), all converge to the point *N* of intersection between *LM* and the chosen ray *1*. This intersection lies closer to the plate than *B*. In this way mainly astigmatism and slight coma occur [2]). These faults can be compensated by introducing a separate optical element, but that would mean that, for instance, a cylindrical lens would have to be placed in the path of the rays to correct the astigmatism. H. de Lang, of the Philips Laboratory at Eindhoven, has shown [3]) that a compensation can be achieved merely by altering the form of the glass plate slightly. The front surface must remain plane because of the mirror action, but if the plate is made slightly wedge-shaped or if the back surface is ground weakly convex, the aberrations can be suppressed to a great extent. For a television camera with a plate a few mm thick at an angle of 45° to the light beam, a prism angle of 7′ or a radius of curvature of 8 m for the back surface is sufficient.

In the third place, the thickness of the glass introduces difficulties in the crossed arrangement of the mirrors. If one uses the system shown in fig. 12, the mirror *b* must be interrupted to allow mirror *r* to pass through and therefore no blue

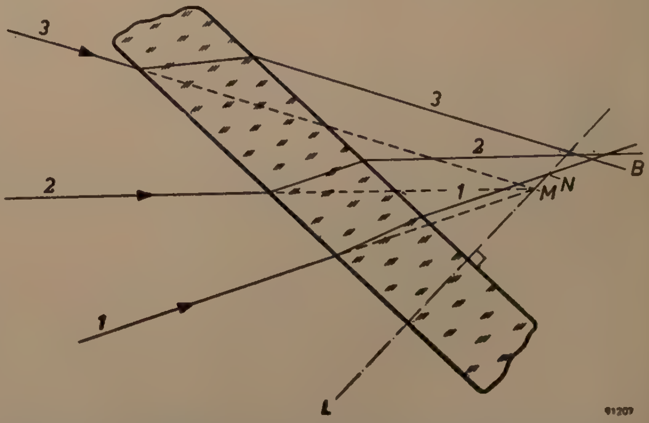

Fig. 13. The thickness of the glass of the semi-reflecting mirror produces aberrations in the transmitted beam: the rays *1*, *2* and *3* converging towards *M* no longer intersect in one point after passing through the mirror.

---

[2]) For these optical aberrations see e.g. W. de Groot, Philips tech. Rev. **9**, 301-308, 1947/48.

[3]) See Philips Res. Rep. **12**, 181-189, 1957 (No. 3).

light would be reflected where the cross-over occurs. A construction as shown in *fig. 14a* is thus usually preferred. The thickness of the glass means that the boundary *AB* forms an irregularity which can intercept light, as in the case of ray *1*. Such a cross is therefore usually placed in a position in the apparatus where the rays travel as far as possible parallel to the plane *AB*, e.g. parallel to the optical axis: ray *2* in fig. 14*a* is not intercepted, but the rays which do not travel parallel to the axis (originating for example from the top and bottom edges of the object to be reproduced), like ray *1*, may be partly intercepted and shadow-formation by plane *AB* may occur. This can be prevented by making the first mirrors (r_1, b_1) thicker than those behind (r_2, b_2; fig. 14*b*): refraction in the thicker mirrors displaces the beam so far laterally that no light falls on the dividing surface between the back mirrors. This method, however, is only permissible for objects which are apparently at an infinite distance, because otherwise each image point would be doubled.

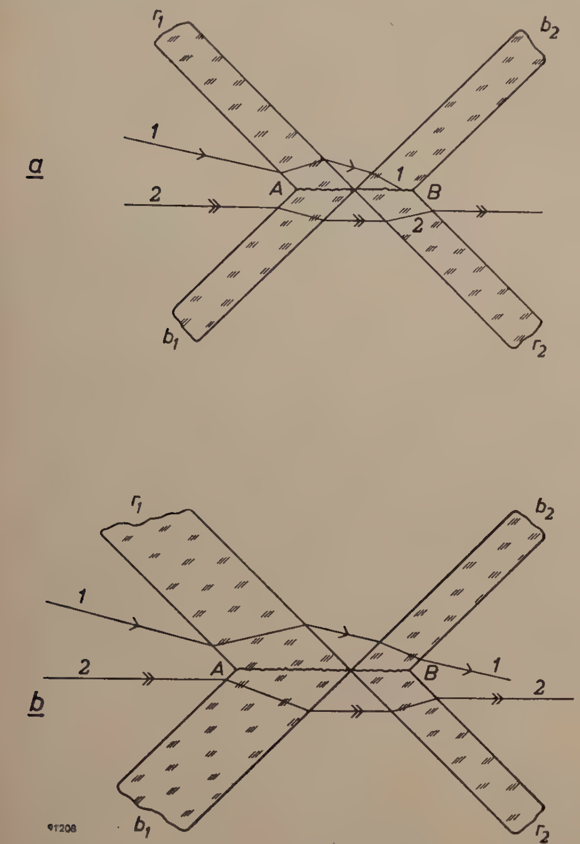

Fig. 14. r_1r_2-b_1b_2 are dichroic mirrors in an arrangement differing slightly from that in fig. 12. In (*a*) ray *2* which enters parallel to the boundary plane *AB*, can pass unhindered, but the obliquely incident ray *1* is lost in *AB*. In (*b*) the first mirrors (r_1 and b_1) are made so thick that ray *1* is laterally displaced far enough to avoid *AB*.

Summary. The well-known phenomenon of the interference of light in thin films has found many practical applications in recent years. According as the refractive index of the film is higher or lower than that of the carrier substance, the film increases or reduces the reflection. The magnitude of the effect depends on the relationship between the thickness of the film and the wavelength of the light used. By a suitable combination of layers, the effect can be enhanced and in this way practically loss-free mirrors can be prepared which transmit one region of the visible spectrum and reflect another region (dichroic mirrors). The preparation of such layers by sublimation in vacuum and the application of dichroic mirrors in colour television are discussed.

A HIGH-PRECISION LATHE HEADSTOCK

621.941.26-229.331

Lathes for machining with high precision in a direction perpendicular to the axis of rotation are generally available. On special toolroom lathes shafts may be turned to a diameter tolerance of a few microns, whilst local surface roughness may even be reduced to e.g. $\frac{1}{2}$ μ.

Whenever a lathe is used to machine flats or profiles on end surfaces, e.g. plastic lenses, we are concerned with the accuracy in a direction *parallel* to the axis. This accuracy, which is not very critical for ordinary applications, is mainly dependent upon the thrust bearings of the lathe spindle.

With other machine tools, such as grinding and drilling machines, it may also occur that for obtaining extremely smooth surfaces a highly accurate thrust bearing is desired. Adequate results for this purpose may be reached with conical slide-bearings, but a fairly large tolerance must be observed to allow for changing loads. Clearly this affects the accuracy that can be attained. A bearing free of this drawback and ensuring a very high degree of axial and radial accuracy has been developed in the Eindhoven Research Laboratories. Its construction is shown in *fig. 1.* The end of the main spindle, which is accurately supported in radial direction by the bearing, is fitted with a piece of "improved wood" (*B*). This wooden member rests against a stationary metal thrust block, whose front surface has been lapped plane and perpendicular to the main spindle with a high degree of accuracy. The main spindle is pressed against the thrust block with a *constant force*, owing to the fact that a constant pressure below atmospheric pressure is maintained in the closed compartment *D* in which this contact takes place. The thrust block can be axially displaced by means of a micrometer screw. It this way the workpiece on the main spindle can be displaced over an extremely small distance (the cutting depth) with respect to the tool.

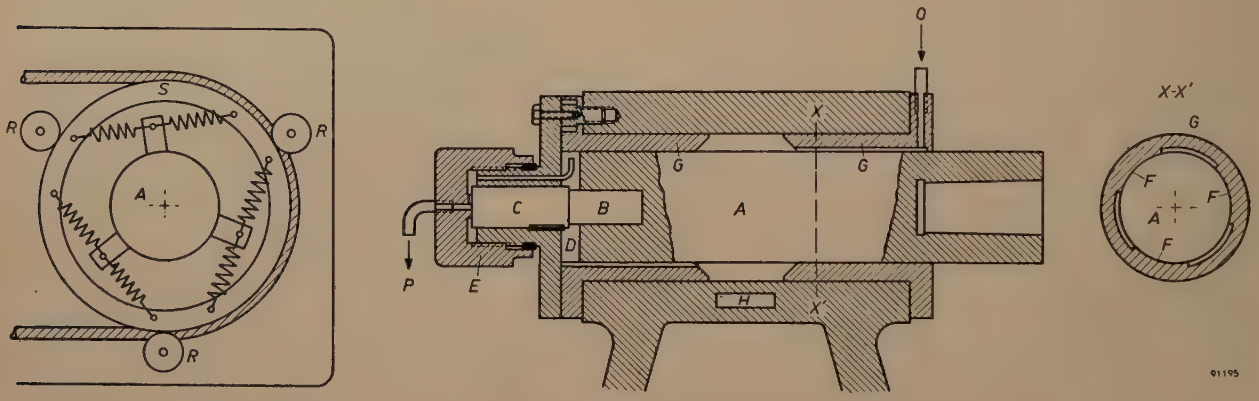

Fig. 1. Construction of the precision headstock. A steel shaft running in bronze bearing block *G* (which has three bearing surfaces *F*, see section *XX'* on right). *B* improved-wood end-piece; *C* metal thrust bearing block, which may be moved axially by means of the micrometer screw *E*. In the space *D* a constant pressure, beneath atmospheric, is maintained. *H* heating element. *O* oil inlet, *P* oil outlet.

The left-hand figure shows the drive. The pulley *S*, connected to the headstock shaft by six springs, runs in three rollers *R* mounted on a bracket attached to the wall of the workshop.

Evidently the position of the tool in axial direction must be fixed with great precision as well, but this requirement can be readily satisfied.

The low pressure in the above compartment also sucks in an ample flow of oil along the main spindle, so that the latter is efficiently lubricated, which is necessary for a very accurate radial support: both the steel spindle and the three supporting surfaces (*F* in fig. 1) of the bronze bearing block have been accurately lapped to size with a tolerance of only about 1 μ. This means that a temperature drop of 5 °C would cause the spindle to seize because of the difference in coefficient of expansion between the two materials. This is avoided by keeping the whole bearing at a constant temperature of about 30 °C with a heating element. The enforced oil-flow prevents any excessive local overheating of the sliding surfaces, which would increase the play.

The spindle should be driven with the greatest uniformity, avoiding any vibrations in the drive.

The pulley is therefore not fitted rigidly to the spindle, but coupled to it via steel springs, the pulley being supported not by the spindle bearing, but on rollers of its own.

The axial accuracy attainable with this construction can be deduced from *fig. 2*, a photo-micrograph of the surface of a flat disc machined on a lathe equipped with the headstock in question. A diamond-tipped tool was used with a round tip of radius 200 μ. The lateral displacement of the tool was 9 μ per revolution. The finished surface thus consists of adjacent grooves 9 μ wide and with a depth of $4.5^2/(2\times 200) \approx 1/20$ μ. A close examination of the photo shows that the width of the groove never varies by more than about 5%. This means that during a short period (the machining of the area shown in the picture lasted about 5 seconds) the axial displacement of the lathe spindle relative to the tool did not amount to more than 10% of the groove depth, i.e. less than 1/200 μ.

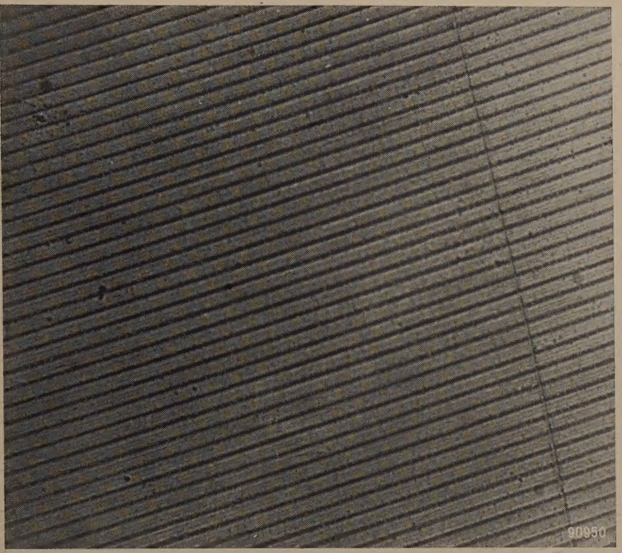

Fig. 2. Photomicrograph (∼250×) of the surface of a disc of plastic material machined flat with a diamond tool on a precision lathe provided with the headstock described here. From the uniformity of the groove width it can be deduced that movement in the axial direction during working was less than 1/200 micron.

The same lathe was used for machining a cavity resonator for 8.75 cm wavelength, earlier described in this Review 1), for high-precision measurements of the dielectric losses in solids. It was essential to keep local unevenness of wall, bottom and cover of the cavity as small as possible with respect to the penetration depth of the H.F. currents, viz. about 1 μ for the wavelength in question. Measurements of the quality factor of the cavity resonator confirmed that the unevenness of the machined surfaces was indeed very small with respect to the penetration depth.

This lathe is now also in use for making the aspherical Schmidt correction plates of mirror cameras for X-ray fluorography 2).

L. M. LEBLANS.

---

1) M. Gevers, Measuring the dielectric constant and the loss angle of solids at 3000 Mc/s, Philips tech. Rev. 13, 61-70, 1951/52.

2) Philips tech. Rev. 13, 269-281, 1951/52. For manufacturing the correction plates of smaller Schmidt systems (e.g. for projection TV sets), a simpler method has been developed; see Philips tech. Rev. 9, 349-356, 1947/48.

ABSTRACTS OF RECENT SCIENTIFIC PUBLICATIONS BY THE STAFF OF N.V. PHILIPS' GLOEILAMPENFABRIEKEN

Reprints of these papers not marked with an asterisk * can be obtained free of charge upon application to Philips Electrical Ltd., Century House, Shaftesbury Avenue, London W.C. 2.

2432: J. de Jonge and H. J. van den Bergh: The preparation of 2,4,6-trimethoxymethyl phenol (Rec. Trav. chim. Pays-Bas **75**, 1214, 1956, No. 9-10).

The preparation of 2,4,6-trimethoxymethyl phenol is described.

2433: P. Jongenburger: De invloed van dislocaties op enige fysische eigenschappen van vaste stoffen (Ned. T. Natuurk. **22**, 297-305, 1956, No. 10). (The effect of dislocations on certain physical properties of solids; in Dutch.)

A review of the effect of dislocations in metals (especially copper) on the electrical resistance and on the increase of resistance in a magnetic field. The effect on nuclear spin resonance is also considered; this is an effect which can be studied also in non-conducting crystals. Measurements of these effects enable the concentration of dislocations to be approximately determined.

2434: J. I. de Jong, R. Dijkstra and J. de Jonge: The ortho/para distribution of methylol groups in the reaction of phenol and formaldehyde, I (Rec. Trav. chim. Pays-Bas **75**, 1289-1302, 1956, No. 9-10).

In the reaction between phenol and formaldehyde in aqueous solution at 90 °C and *p*H = 5.5-6.5, about 58% ortho substitution and 42% para substitution takes place initially. A colorimetric method for the determination of methylol phenols in solution is described.

2435: D. Kleis: Toepassing en opstelling van luidsprekers in geluidsinstallaties (T. Ned. Radiogenootschap **21**, 237-254, 1956, No. 5). (Application and arrangement of loudspeakers in sound installations; in Dutch.)

Speech and music put different requirements on the acoustics of an auditorium, so neither for live performances nor for recordings can the listening conditions be optimum for both. Inadequate acoustical conditions can be corrected both for live performances and recordings by using separate loudspeakers for direct and indirect sound. Loudspeakers for direct sound should have pronounced directivity towards the listeners so as to minimise reverberation. Sound reinforcement or sound transmission by this type of loudspeakers — horns or sound-columns — yields optimum intelligibility of speech; a stereophonic reproduction can fully represent the direct sound of a live performance of speech or music. Loudspeakers around the auditorium, producing diffuse reverberating sound are used to suggest reflections from the walls and to produce the adequate level of indirect sound for music. In order to suggest natural reflections, their signals have to be retarded in accordance with the loudspeaker positions. The acoustics of the auditorium may be controlled by the studio and so be made optimum for any kind of performance by using two-channel transmission or twin-track recordings.

2436: J. H. Stuy: Studies on the radiation inactivation of micro-organisms, IV. Photoreactivation of the intermediate stages in the transformation of *Bacillus cereus* spores into vegetative cells (Antonie van Leeuwenhoek J. Microbiol. Serol. **22**, 337-349, 1956, No. 4).

Continuation from articles I, II & III (these abstracts **2274**, **2428**, **2429**). The transformation of *Bacillus cereus* spores into vegetative cells has been studied. It was possible to distinguish between five different stages. Each stage could be isolated. During the development of stage III cells from stage II spores the phenomenon of photoreactivation could be observed. The results strongly suggest that the non-photoreactivability of UV-inactivated resting spores and stage II spores is due to their limited metabolic activity.

2437: M. G. van der Steeg and K. J. de Vos: Reversibility of the coercive force in Alnico 5 (J. appl. Phys. **27**, 1250, 1956, No. 10).

Interim report on the discovery by means of X-rays of a new face-centered cubic phase in Fe-Co-Ni-Al magnetic alloys. The new phase is observed after long annealing (70 days) of the alloy at 600 °C. As is well known, a growing phase exerts an influence on certain physical properties before its presence can be demonstrated by X-ray diffraction. Magnetic measurements made after much shorter annealing times suggest that the newly discovered phase plays an important part in the achievement of the large coercivity of Alnico 5 (Ticonal G).

2438: L. J. van der Pauw and D. Polder: The photo-thermoelectric phenomenon in semiconductors (J. Electronics **2**, 239-240, 1956, No. 3).

The photo-thermoelectric effect is the phenomenon that the thermoelectric potential between two materials changes when one of the materials is illuminated. For this effect an expression has been derived by Tauc, assuming that the energy difference between the conduction band and the valency band is independent of the temperature. The authors show,however, that Tauc's result is valid only if the mobility of holes and electrons are also independent of the temperature. A new expression is given which takes both temperature dependencies into account. The additional terms in this expression are of the same order of magnitude as Tauc's result.

2439: H. G. van Bueren: Magnetoresistivity of plastically deformed metals (Proceedings of the IUTAM Colloquium on the deformation and flow of solids, Madrid 1955, published by Springer, Berlin 1956, pp. 79-89).

The magnetoresistance at very low temperatures of pure polycrystalline copper has been found to increase considerably, when plotted in a reduced diagram, upon plastic deformation. This effect is due to dislocations, as subsequent annealing up to 220 °C has no effect whatever on the additional relative magnetoresistivity. Neither vacancies and interstitials nor impurity atoms effect the relative magnetoresistance, and the latter quantity forms therefore a suitable tool to study dislocations separately. A theory is outlined, according to which the anisotropic scattering by dislocations is the main cause of the phenomenon. The numerical agreement between the result of this theory and the observations is satisfactory.

2440: F. A. Kröger and H. J. Vink: Relations between the concentrations of imperfections in crystalline solids (Solid State Physics, **3**, editors F. Seitz and D. Turnbull, pp. 307-435, Academic Press, New York 1956).

A number of properties of crystalline solids such as the electronic or ionic conductivity, the colour, the luminescence, the magnetic susceptibility, are determined by the presence of imperfections, viz. free electrons and holes, vacant lattice sides, interstitial atoms, and foreign atoms. The concentrations of these imperfections are not independent of each other. In the present paper a quantitative discussion is given of the relations existing between the various imperfections. Mainly complete equilibrium (corresponding to high temperature) is discussed. Starting from this state, possibilities for incomplete equilibrium (as may be present after cooling) are also considered. The discussion covers *a*) pure compounds having a composition corresponding to a simple stoichiometric ratio, *b*) compounds showing a deviation from the simple stoichiometric ratio, *c*) compounds containing one or more types of foreign atoms. With the aid of the theory given — which is based on the theory of imperfections of Schottky and Wagner — it is possible to give a quantitative interpretation of the intricate relation existing between the conditions of preparation of crystals, and their electrical, optical and magnetic properties. A special aspect of these relations is the interdependence of the solubilities of foreign atoms.

2441: B. D. H. Tellegen: La recherche pour une série complète d'éléments de circuit idéaux non-linéaires (Rendiconti del seminario matematico e fisico di Milano **25**, 134-144).

The five ordinary circuit elements (resistance, inductance, capacitance, transformer, gyrator) can be considered, by definition, to represent the simplest linear constant passive systems. From a physical point of view, linear constant active systems, linear variable systems, and non-linear systems all belong to the class of non-linear constant passive systems. The search for the simplest non-linear constant passive systems leads to ideal non-linear net-work elements. For order zero these are the ideal rectifier, the elements called voltage sink and current sink, and four ideal amplifiers.

2442: H. G. van Bueren: Dislocaties in niet-metalen (Ned. T. Natuurk. **22**, 394-402, 1956, No. 12). (Dislocations in non-metals; in Dutch.)

Dislocations have much more influence on the physical properties of alkali-halides and semiconducting elements than on those of metals. They can act as sources of vacancies, and therefore of colour centres, in ionic crystals, which explains the enhanced colouring by X-ray irradiation of previously cold-worked crystals, and the equally enhanced conductivity. In germanium, dislocations produce acceptor levels and reduce the carrier mobility. The motion of dislocations in valence type crystals, is impeded by the typical core structure of the imperfections, which is characterized by the occurrence of unpaired bond electrons.

2443: J. Bloem, A. J. van der Houven van Oordt and F. A. Kröger: A new luminescence emission in Cu_2O (Physica **22**, 1254-1256, 1956, No. 12).

Cu_2O is known to show luminescence in the infra red near 1 μ. In the present investigation it is shown that at 20 °K this emission consists of two sub-bands at 0.91 and 1.01 μ. Samples prepared at 960 °C under oxygen pressures of 10^{-1}-10^{-3} mm Hg show in addition two luminescence peaks at shorter wavelengths, viz. 0.72 μ and 0.82 μ. The former bands are attributed to copper vacancies, the latter to oxygen vacancies.

2444: J. A. Kok and M. M. G. Corbey: Breakdown of liquid insulating and dielectric material (Appl. sci. Res. **B6**, 197-206, 1956, No. 3).

One of the possible causes of long-time breakdown of low-frequency impregnated paper capacitors and cables is known to be the long-time formation of a conducting bridge between the electrodes, followed by a short-time thermal breakdown. Such a bridge may consist of polarizable particles, ions or colloidal contaminants of high dielectric constant, particularly conducting material. These particles flow towards a place of maximum stress because of the action of transverse quadratic gradient forces in a non-uniform field, thus forming a conducting path for the short-time development of gas and the subsequent breakdown by ionization. From a long-time breakdown strength of 50 kV/mm there follows a particle diameter of about 30 Å.

2445: J. A. Kok: Theory and probe measurements of Gabor's gas-filled triode (Appl. sci. Res. **B6**, 207-221, 1956, No. 3).

By means of a number of probe measurements in Gàbor's gas-filled triode with a spread dark discharge in the cathode chamber, the form of the characteristic I_a-V_a curves was established and several relations between various quantities derived. With these results it was possible to calculate a relation between Gàbor's and Fetz's criteria of the transition of the spread discharge into a constricted one.

2446: J. Ugelstad and J. de Jonge: The alkaline hydrolysis of alkoxymethyl ureas (Acta chemica scandinavica **10**, 1475-1487, 1956, No. 9).

Alkoxy methyl ureas, surprisingly enough, were found to be quite readily hydrolysed in moderately alkaline solution at room temperature, giving urea formaldehyde and an alcohol as end products. The decomposition of different alkoxymethyl ureas was investigated kinetically. The hydrolysis was found to be proportional to the OH-ion concentration. Based on kinetic investigations in strongly alkaline solution, a choice is made between two possible reaction paths for the reaction. It may be concluded that the reaction involves the breaking of an other bond, i.e. that methylol urea and alcohol are the first decomposition products. The reaction is specific for ethers of methylol urea, ethers of methylol compounds of carboxylic acid amides being comparatively very stable in alkaline solution. The reaction mechanism is discussed.

R 314: H. de Lang: Compensation of aberrations caused by oblique plane-parallel plates (Philips Res. Rep. **12**, 181-189, 1957, No. 3).

Methods are given for the correction of aberrations (astigmatism and coma) introduced by an oblique plane-parallel plate in a convergent beam. It is shown that astigmatism can be eliminated, either by giving the plate a slight amount of prismaticy or by giving the rear surface of the plate a slight amount of spherical or cylindrical curvature. In practical cases the first method is preferable as it avoids cylindrical surfaces and also nearly eliminates coma. Off-axis correction of astigmatism impose the extra condition that the derivative of the astigmatism in the meridional section be zero. It is shown that in general this on-axis correction can be achieved by a suitable combination of prismaticy and curvature.

R 315: H. G. van Bueren: Influence of lattice defects on the electrical properties of cold-worked metals (Philips Res. Rep. **12**, 190-239, 1957, No. 3).

Continuation of **R 306.**

R 316: W. Ch. van Geel and B. J. J. Schelen: Some properties of oxide layers produced on aluminium by electrolytic oxidation (Philips Res. Rep. **12**, 240-248, 1957, No. 3).

A description is given of measurements of the thickness (d), dielectric constant (ε) and density (ϱ) of oxide layers produced on Al by electrolytic oxidation. The X-ray investigation of the structure of these layers was also undertaken. Two different values were found for the thickness of the layer, viz. $d = 13.7$ Å/volt and $d = 12.7$ Å/volt. The former value was found after chemical cleaning, the latter without any prior removal of the oxide layer formed by reaction with the air. The cleaning probably causes an increase of about 7% in the surface area. If this is correct, then $d = 12.7$ Å/volt is the more acceptable value. For ϱ we found the value 3.1 g/cm^3, for ε the value 8.7. When it is formed at room temperature, the oxide is completely amorphous, except when a layer of boehmite has been produced on the Al by boiling it in water. In the latter case γ'-Al_2O_3 is also formed. Oxidation at 100 °C always gives some γ'-Al_2O_3 as well as amorphous Al_2O_3.

R 317: J. L. H. Jonker: On the theory of secondary emission of metals (Philips Res. Rep. **12**, 249-258, 1957, No. 3).

The angular distribution of the secondary emission of nickel is measured with small intervals of energy. The results allow us to make a hypothesis about the mechanism of the emission, about the energy distribution, and about the scattering of secondary electrons inside the metal. An explanation is proposed for the cosine distribution of the emitted electrons.

R 318: K. F. Niessen: On a higher approximation of the critical field strength for an antiferromagnetic (Philips Res. Rep. **12**, 259-269, 1957, No. 3).

The critical magnetic field strength is derived for an antiferromagnetic with different anisotropy constants for the two sublattices, account being taken of the field-strength dependence of the parallel and perpendicular susceptibilities and a higher approximation of the anisotropy energy. Special attention is paid to the variation of the critical field strength for a small deviation of the external field from the preferential axis. Formulae (20) and (21) contain the results for the case of equal and (25) and (27) for the case of unequal anisotropy constants.